

Development of a Digital Computer Model of the
Coronary Circulation.

by

Laurence Ray Simar jr.

Bioengineering

Submitted in Partial Fulfillment of the Requirements of the
University Undergraduate Fellows Program

1980-1981

Approved by:

Walter S. Kuklinski

W. S. Kuklinski

April 1981

ABSTRACT

Development of a Digital Computer Model of the
Coronary Circulation.

Laurence Ray Simar jr.

Advisor: Dr. Walter Kuklinski

A model of the coronary circulation which includes the effect of ventricular contraction is developed. A fluid/electrical analog is used. The analog incorporates the effects of ventricular contraction with a voltage source. Collapse of the coronary arteries during ventricular contraction is incorporated into the model. The resulting trends in arterial flow, pressure, and cross sectional area are reasonable and appear to be compatible with published data.

ACKNOWLEDGMENTS

I acknowledge with much appreciation the patience and guidance of Dr. Kuklinski throughout the year. I am grateful to Karen for her understanding, help, and concern during this endeavor. My greatest appreciation goes to my Mom and Dad for their love and support.

TABLE OF CONTENTS

INTRODUCTION	1
MODEL DEVELOPMENT	2
METHODS	35
RESULTS	43
DISCUSSION	60
REFERENCES	62
APPENDIX	64
VITA	75

LIST OF TABLES

1. Values of R, L, C for circular and
elliptical cross section 27
2. Fluid and electrical analogs 29

LIST OF FIGURES

1.	The coronary vessels	3
2.	Muscle fibre orientation in wall of left ventricle	6
3.	Stress ratios in left ventricle at end of diastole and systole	7
4.	Variation of apparent viscosity of human blood with rate of shear	9
5.	Incremental Young's modulus and dis- tending pressure vs. diameter for a piece of artery of fixed length	11
6.	Transverse cross section of a flexible tube as a function of transmural pressure	13
7.	Linearized representation and cut off ratios for cross sectional configuration	14
8.	Flat velocity profile approximation for circular cross section	19
9.	Segment of a thin walled tube	21
10.	Radial wall displacement of a thin walled tube	22
11.	Flat velocity profile approximation for elliptical cross section	26
12.	(a) Section of artery. (b) L net- work lumped equivalent circuit	31

13.	(a) Section of coronary artery.	
	(b) L network lumped equivalent circuit	33
14.	L network lumped equivalent circuit for a dumbbell cross section	37
15.	Generalized flow chart for coronary blood flow model	39
16.	Implemented model of a coronary arterial segment	40
17.	Aortic and ventricular pressure waveforms	42
18.	General trends of R, L, C as a function of area	44
19.	External pressure in each section for simultaneous contraction	45
20.	External pressure in each section for phased contraction	47
21.	Transient and forced response flow curves	48
22.	Sectional pressures for simultaneous ventricular contraction	49
23.	Sectional flows for simultaneous ventricular contraction	50
24.	Sectional areas for simultaneous ventricular contraction	51

25.	Sectional pressures for phased ventricular contraction	52
26.	Sectional flows for phased ventricular contraction	53
27.	Sectional areas for phased ventricular contraction	54
28.	Modelled and measured flows for the left coronary artery	58
29.	Modelled and measured flows for the left circumflex coronary artery	59
30.	Half-interval method	67

I. INTRODUCTION

Considerable advances have been made in the area of hemodynamics in the past several years. Physicians and engineers have worked together to develop mathematical models dealing with various portions of the circulatory system. These models have dealt with most aspects of both venous and arterial circulation. The coronary circulation has received far less attention. The reason for this lack of development is due to the complexities of the coronary circulation. A well developed model of the coronary circulation would provide the diagnostician with a valuable tool. A model would allow for accurate prediction of blood flow to various regions of the heart and for an accurate description of the effect of atherosclerosis and other types of coronary arterial disease on blood flow. The researcher could more accurately analyze the effects of drugs on coronary blood flow by using information the model could provide about the effects of ventricular contraction on coronary blood flow. The purpose of this thesis is to develop a model of the coronary circulation which takes into account the effect of ventricular contraction on coronary blood flow.

IEEE Transactions on Biomedical Engineering was used as a pattern for format and style.

II. MODEL DEVELOPMENT

Morphology of Coronary Circulation

Before developing a model of the coronary circulation, it is important to understand the morphology of the coronary circulation. Two main coronary arteries, the left and right, arise near the aortic valve (Fig. 1). The left coronary artery supplies the left ventricle and the anterior half of the septum. The right coronary artery supplies the right ventricle and the posterior half of the septum. There are many anastomoses of the two systems at the apex. These anastomoses act as a safety factor by reducing the area of ischemia when one of the arteries is occluded. The blood flow in the left coronary is comparable to that in the right coronary artery, 880 ml per 100 gm of left ventricle per minute. The total flow may amount to 5% of the resting cardiac output (1).

The primary divisions of the left coronary artery, the anterior descending and circumflex arteries, give rise to an anastomosing plexus of vessels. The subepicardial networks give rise to two kinds of vessels. First, there are vessels which form subsidiary networks of anastomosing vessels arranged parallel to the surface of the heart. From these arise precapillaries giving rise to the capillaries supplying the outer portion of the myocardium. Secondly, there are vessels which branch initially at an acute angle to the horizontal line of the parent vessels then plunge vertically down through the thickness of the myocardium. Some of these vessels have a short course and divide within the thickness of the myocardium; others run with little

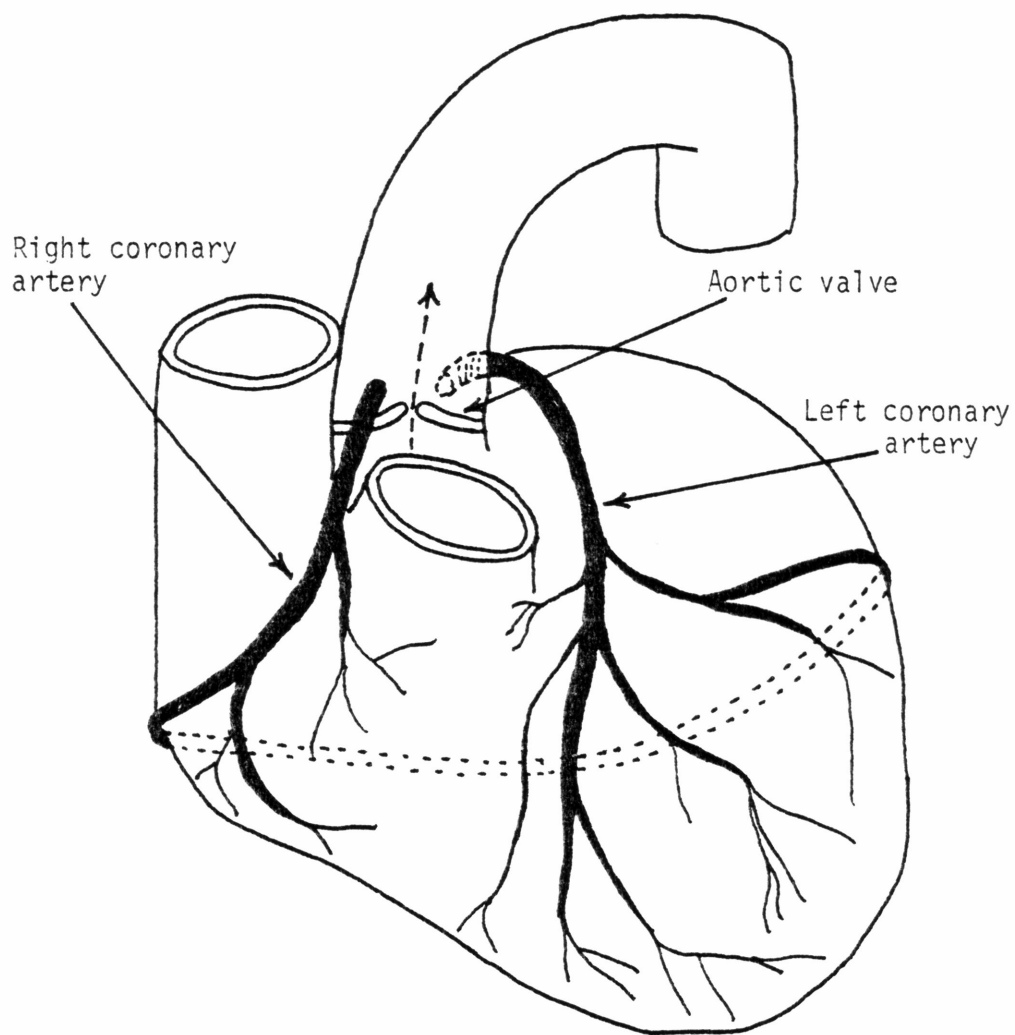


Fig. 1. The coronary vessels (1).

intermediate branching to the subendocardial surface. The subendocardial branches of the perforating vessels form a complex network of vessels. The branches may run relatively lengthy distances, branching and giving rise to precapillary vessels en route (2).

Capillaries are distributed throughout the myocardium. The capillaries form parallel sheets of anastomosing vessels in the thickness of the myocardium. The subendocardial sheets of capillaries are very similar in arrangement to the subepicardial surface (2).

The primary venule is formed by the junction of varying numbers of venous capillaries. The venules run a very short course before joining their neighbors and rapidly expand into veins of varying dimension. Most veins join to form drainage veins which travel in close relationship to the arteries, usually in a pattern of two veins flanking one artery (2).

Effects of Ventricular Contraction

The greatest obstacle to the investigation of coronary flow has been the very marked mechanical effect of ventricular contraction on the cross sectional configuration of the coronary vessels that run within the contracting muscle. Contraction is accompanied by a rise in tissue pressure dependent upon the location of the coronary vessel in the wall. The increase in tissue pressure surrounding the vessels reduces their transmural pressure and in the case of the left coronary vessels, temporary occlusion occurs. Therefore, the resistance to flow of the coronary vascular bed changes greatly throughout the cardiac cycle (1). The effect of transmural pressure on the vessel

configuration is much more marked and of more interest in the left ventricle.

Since the mechanism resulting in changes in cross sectional configuration is the same in the wall of the left ventricle as in the wall of the right ventricle, it is sufficient to initially examine only what occurs in either the wall of the left or right ventricle. Because of its great importance to the systemic circulation, the left ventricle has been extensively analyzed in the areas of left coronary arterial flow and wall stresses. For these reasons, the model developed will deal only with the portion of the coronary circulation supplying the left ventricle.

The development of stress in the myocardium has been studied by a number of investigators. The main problem involved in models of the left ventricle is the continuous variation of myofibril orientation throughout the myocardium (Fig. 2). The most effective model of the left ventricle to analyze myocardial stresses was developed by Streeter et. al. (4). This study assumed that the ventricle is ellipsoidal and that the muscle-fibers can only bear tension axially. Fibre-orientation was measured in post-mortem canine hearts. These results were used to calculate the distribution of normal and radial stresses through the wall, treating the wall as a tethered set of nested ellipsoidal shells, each shell having a single fibre-orientation which corresponds to the experimentally determined orientation of that level in the wall. The stress ratios calculated by this model in the left ventricular wall at the end of diastole and at the end of systole are shown in Fig. 3. The importance of allowing

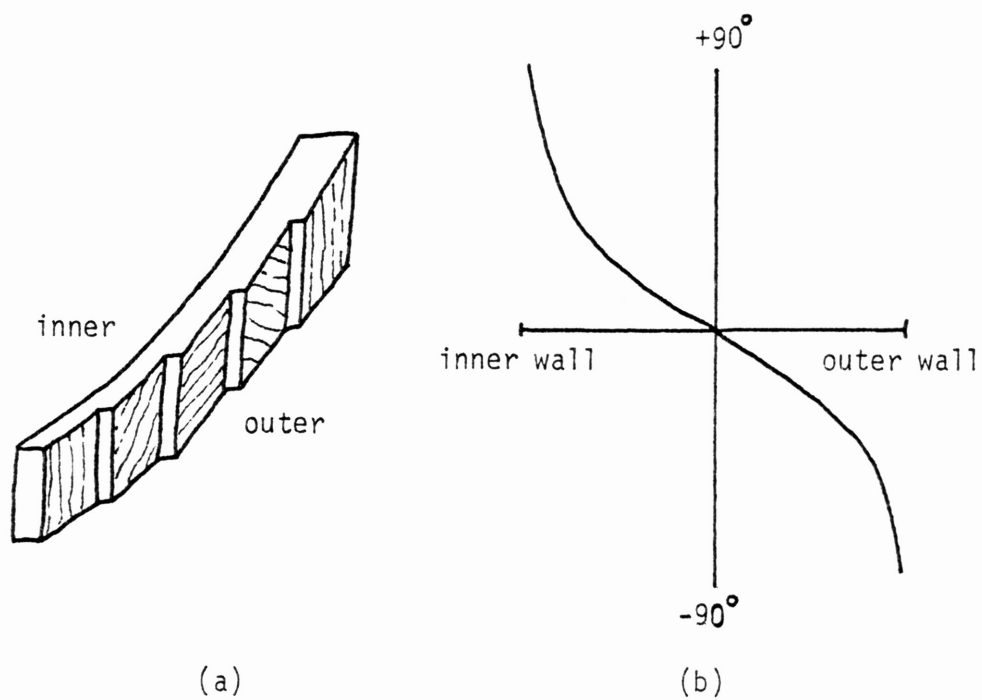


Fig. 2. Muscle fibre orientation in wall of left ventricle.

(a) Orientation of long axis of fibers at successive depths.

(b) Angle of fibre with circumferential plane of left ventricle (3).

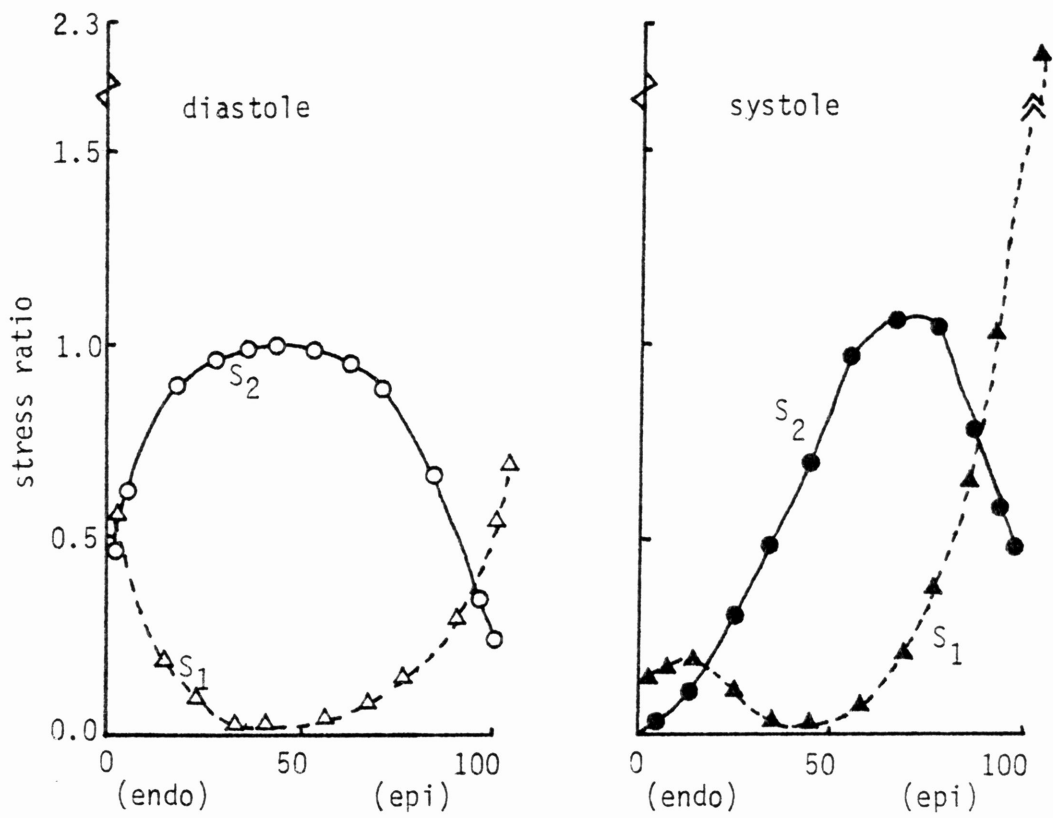


Fig. 3. Stress ratios in left ventricle at end of diastole and systole. S_1 -longitudinal stress, S_2 -circumferential stress (4).

for fibre-orientation in studies of this kind is apparent; in models which assume homogenous wall-properties, both longitudinal (S_1) and circumferential (S_2) stresses are found to be highest at the endocardial surface.

Blood Rheology

Since blood flow through the coronary circulation is being analyzed, it is important to examine the properties of blood. The two properties of interest are viscosity and density.

Blood is identified as a non-Newtonian fluid. A Newtonian fluid is one for which the shear stress is proportional to shear strain rate

$$\tau = \eta \dot{\gamma}$$

where τ = shear stress

$\dot{\gamma}$ = shear strain rate

η = viscosity

Viscosity is defined as a constant and is independent of shear strain rate. However, in the case of blood, there are variations of viscosity with shear rate (Fig. 4). The viscosity of blood increases greatly with increasing hematocrit (1). At normal hematocrit levels the rheology of blood is dominated by the interaction of fibrinogen with red blood cells (5). At shear rates above 1000/s, which is typical for many blood vessels in vivo, non-Newtonian characteristics of blood become insignificant and viscosity approaches an asymptotic value of 3-4 mN s/m² (3). When the blood vessels of interest are sufficiently small that the particulate structure of blood can no longer be ignored (100 μ m diameter), then it is not correct to assume

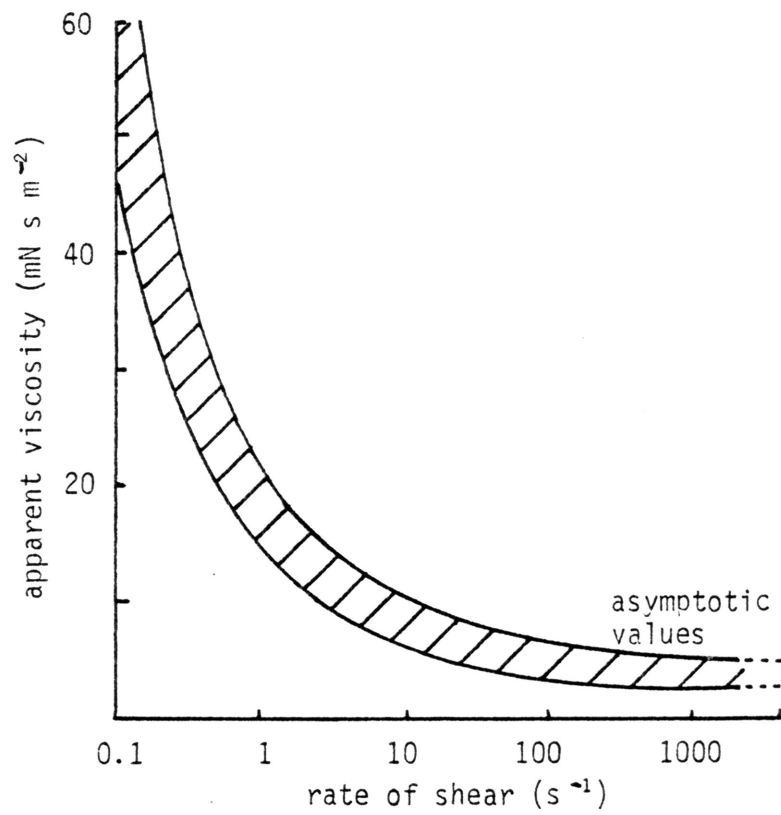


Fig. 4. Variation of apparent viscosity of human blood with rate of shear (3).

blood to be Newtonian (3). The density of blood is 1.05 g/cm^3 (3).

Elastic Properties of Arterial Walls

The properties of the blood vessel walls of the coronary circulation are of great importance to the development of a model of the coronary circulation. This is due to the changes in cross sectional area found in the coronary arteries during the cardiac cycle and the changes in cross section related to pressure differences. The non-linear elastic curve for arteries is well known. Evidence exists that the arterial wall is anisotropic. This is probably due to the different orientations and elastic properties of elastin and collagen (6). The incremental Young's modulus relates circumferential stress to circumferential strain. A graph of the incremental Young's modulus vs. diameter for an artery of fixed length is shown in Fig. 5. It is postulated that elastin causes the low strain part of the curve, while collagen is stressed at the higher strains. The elastic properties of arteries differ in different parts of the arterial system. There are also differences associated with age, disease, and species (6). The aorta has an incremental Young's modulus of approximately $5 \times 10^6 \text{ dyne/cm}^2$ (3).

Cross Sectional Configuration Determination

The variations in vascular bed resistance, as noted previously, are due to changes in cross sectional configuration and area. Katz et. al. analyzed the relationship between cross sectional area and transmural pressure (7). Typical transverse cross sections are shown

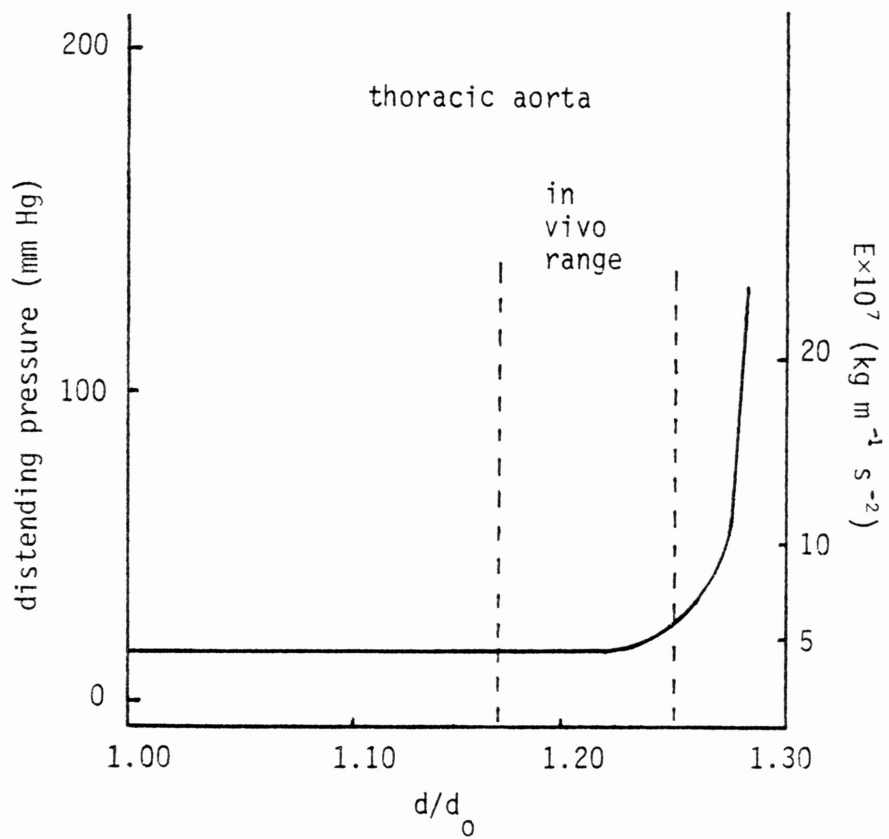


Fig. 5. Incremental Young's modulus and distending pressure vs. diameter for a piece of artery of fixed length. d_0 = unstretched diameter (3).

at various points on the curve in Fig. 6. An approximation to this curve is used in the development of this model of the coronary blood flow. Cross section number three is short lived and acts only as a transient between the elliptical and dumbbell configurations. Therefore, it will be ignored. The linearized representation and the cut off ratios for the cross sectional configurations are shown in Fig. 7. Flow impedance characteristics for the circular cross section have already been determined by other investigators. The impedance characteristics for the elliptical cross section will be determined in this paper. The impedance characteristics of each lobe of the dumbbell configuration are identical to that for a circular cross section.

By examining Fig. 7 the cutoff ratios for various cross sectional configurations can be determined.

$$\text{circular range} \quad \frac{A}{A_0} \geq A_E = \frac{9}{10} \quad (1)$$

$$\text{elliptical range} \quad \frac{9}{10} = A_E > \frac{A}{A_0} \geq A_D = \frac{3}{10} \quad (2)$$

$$\text{dumbbell range} \quad \frac{A}{A_0} < A_D = \frac{3}{10} \quad (3)$$

where A_0 = circular area with no collapse or expansion

A_E = elliptical/circular cut off ratio

A_D = dumbbell/elliptical cut off ratio

A = present cross sectional area

There is a specific advantage to this linearization of cross sectional area change. Without this technique the analysis of cross sectional change would become a very difficult problem of cylindrical shell theory. Linearization avoids this difficulty, greatly reduces

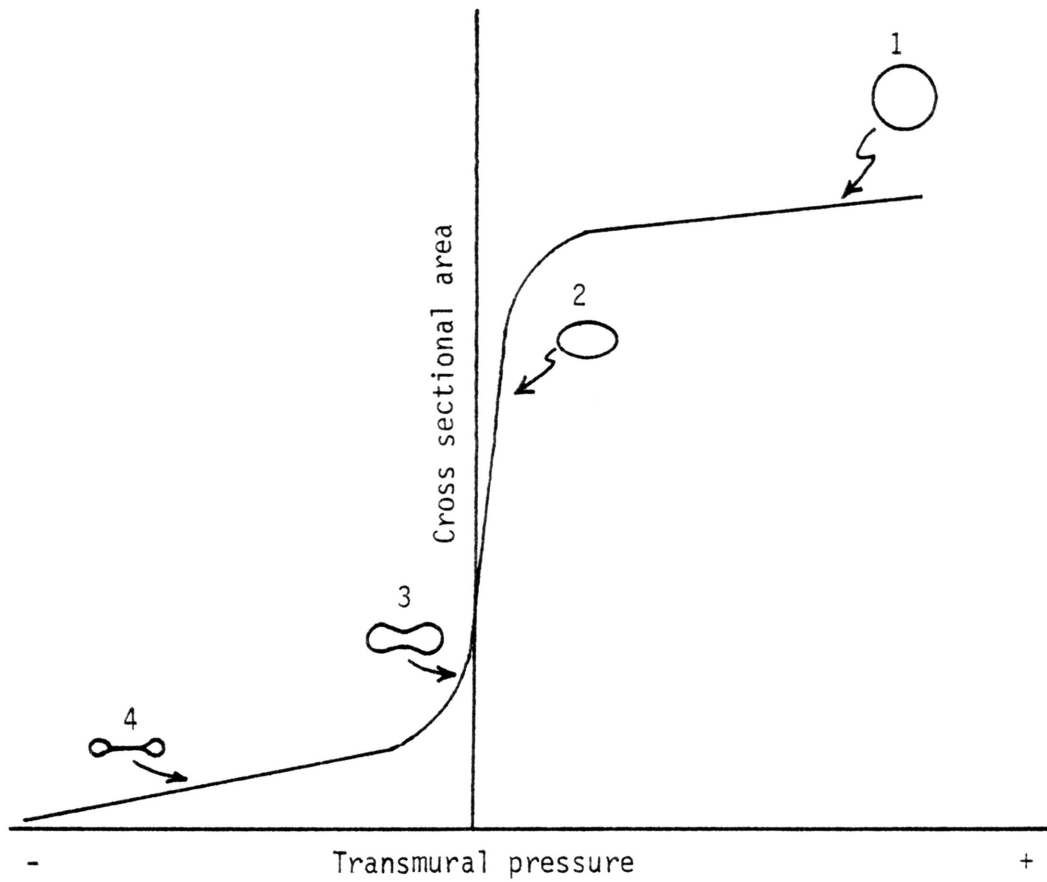


Fig. 6. Transverse cross section of a flexible tube as a function of transmural pressure (7).

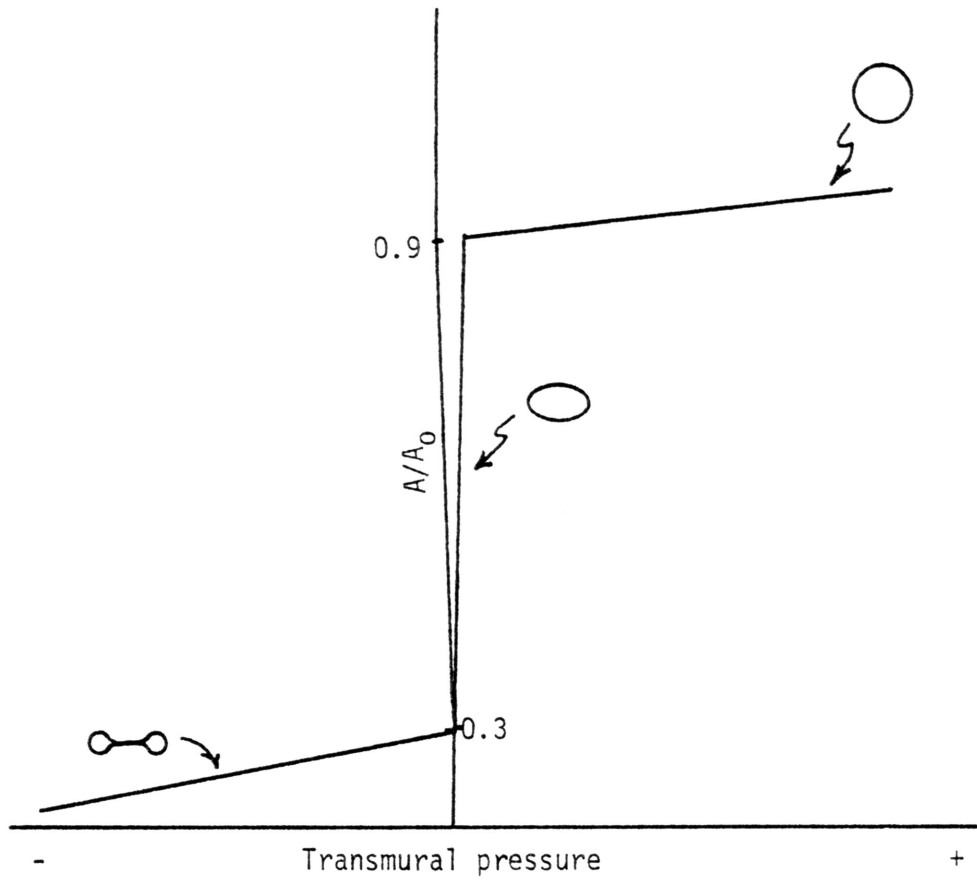


Fig. 7. Linearized representation and cut off ratios for cross sectional configuration.

the complexity of the problem, and accurately describes the system. However, to be totally accurate, the cut off cross sectional ratios would have to be determined using a section of tubing with characteristics as similar as possible to the tube section being modelled; in this case a section of coronary artery.

Governing Equations

The Navier-Stokes equations describe laminar flow of a Newtonian fluid. If body forces (such as those due to gravity) are disregarded and no tangential motion is assumed, then the cylindrical coordinate form of these equations is

$$\begin{aligned} \frac{\partial P}{\partial z} = & -\rho \left(\frac{\partial U_z}{\partial t} + U_r \frac{\partial U_z}{\partial r} + U_z \frac{\partial U_z}{\partial z} \right) \\ & + \mu \left(\frac{1}{r} \frac{\partial}{\partial r} \left(r \frac{\partial U_z}{\partial r} \right) + \frac{\partial^2 U_z}{\partial z^2} \right) \end{aligned} \quad (4)$$

$$\begin{aligned} \frac{\partial P}{\partial r} = & -\rho \left(\frac{\partial U_r}{\partial t} + U_r \frac{\partial U_r}{\partial r} + U_z \frac{\partial U_r}{\partial z} \right) \\ & + \mu \left(\frac{\partial}{\partial r} \left(\frac{1}{r} \frac{\partial}{\partial r} (r U_r) \right) + \frac{\partial^2 U_r}{\partial z^2} \right) \end{aligned} \quad (5)$$

where P = pressure

z = distance along the axis

ρ = fluid density

μ = viscosity

U_z = longitudinal velocity

U_r = radial velocity

Another expression of interest is the continuity equation expressing conservation of mass. If blood is assumed to be incompressible this equation becomes

$$\frac{\partial U_r}{\partial r} + \frac{U_r}{r} + \frac{\partial U_z}{\partial z} = 0 \quad (6)$$

The assumption that blood behaves as a Newtonian fluid has given good results in several other models of blood flow (8-10).

Circular Cross Section Impedance Characteristics

The importance of blood viscosity and density and elastic properties of the arterial walls will become even more apparent during this portion of the derivation of the coronary circulation model. According to Attinger and Attinger (11) no matter what analytical approach is chosen to analyze circulatory flow the impedance consists of two components, a longitudinal impedance (a function of the inertial and viscous properties of the blood) and a transverse impedance (a function of the mechanical properties of the vessel wall). The derivation of these three factors will be based, to some extent, on techniques used by Rideout and Dick (12). The techniques used herein are more straight forward, easily applicable to the cross sectional shapes of concern, and provide results consistent with those of Rideout and Dick.

The first derivation deals with the effect of viscosity on flow. In the case of Poiseuille flow the following additional assumptions are made:

1. steady flow
2. uniform flow
3. symmetric flow

Assuming Poiseuille flow and a circular cross section, equations (4-6) give a velocity profile (U_z) as

$$U_z = \frac{1}{4\mu} \frac{dP}{dz} (r_i^2 - r^2) \quad (7)$$

where P = pressure

z = distance along the tube

μ = viscosity

r = radius of the vessel

r_i = radius of interest

The volumetric flow rate (Q) is given as

$$Q = \int_A U_z dA \quad (8)$$

Substituting equation (7) into (8) and integrating yields

$$Q = \frac{\pi r^4}{8\mu} \frac{dP}{dz} \quad (9)$$

Rewriting equation (9) in difference form yields

$$\Delta P = \frac{8\mu\Delta z}{\pi r^4} Q \quad (10)$$

A resistance (R) relating ΔP and Q can be written as

$$R = \frac{8\mu\Delta z}{\pi r^4} \quad (11)$$

where $\Delta P = QR$

The value of resistance derived by Rideout and Dick is

$$R = \frac{81\mu\Delta z}{8\pi r^4}$$

This fluid resistance is only 81/64 times larger than that given by Poiseuille's law. Studies performed on a model of the arterial system showed that the resistance term of Rideout and Dick could be optimized by a multiplicative constant (10). Therefore the differences between assuming Poiseuille resistance and using the resistance term derived by Rideout and Dick are negligible. This

derivation gives the effect of viscosity on the longitudinal impedance.

The relationship between inertial effects and longitudinal impedance will now be examined. In this case the assumptions made are

1. uniform flow
2. symmetric flow

Returning to the Navier-Stokes equations (4-6) yields

$$\frac{dU_z}{dt} = \frac{1}{\rho} \frac{dP}{dz} \quad (12)$$

Rearranging equation (12) gives the velocity profile (U_z)

$$U_z = \frac{1}{\rho} \frac{dP}{dz} \int dt \quad (13)$$

The flow rate (Q) is given as

$$Q = \int_A U_z dA \quad (14)$$

Substituting equation (13) into (14) yields

$$Q = \frac{1}{\rho} \frac{dP}{dz} \iint_A dA dt$$

Rideout and Dick assumed a flat velocity profile as shown in Fig. 8. This gives a zero velocity beyond $R = \frac{2r}{3}$. Since the velocity profile found in the arterial system is basically flat (3) and the velocity always drops off at the edges of the tube (12), this velocity profile is a reasonable approximation. Evaluating the integral over this cross section area gives

$$Q = \frac{4}{9} \frac{\pi r^2}{\rho} \frac{dP}{dz} \int dt \quad (15)$$

Taking the derivative of equation (15) with respect to time yields

$$\frac{dQ}{dt} = \frac{4}{9} \frac{\pi r^2}{\rho} \frac{dP}{dz} \quad (16)$$

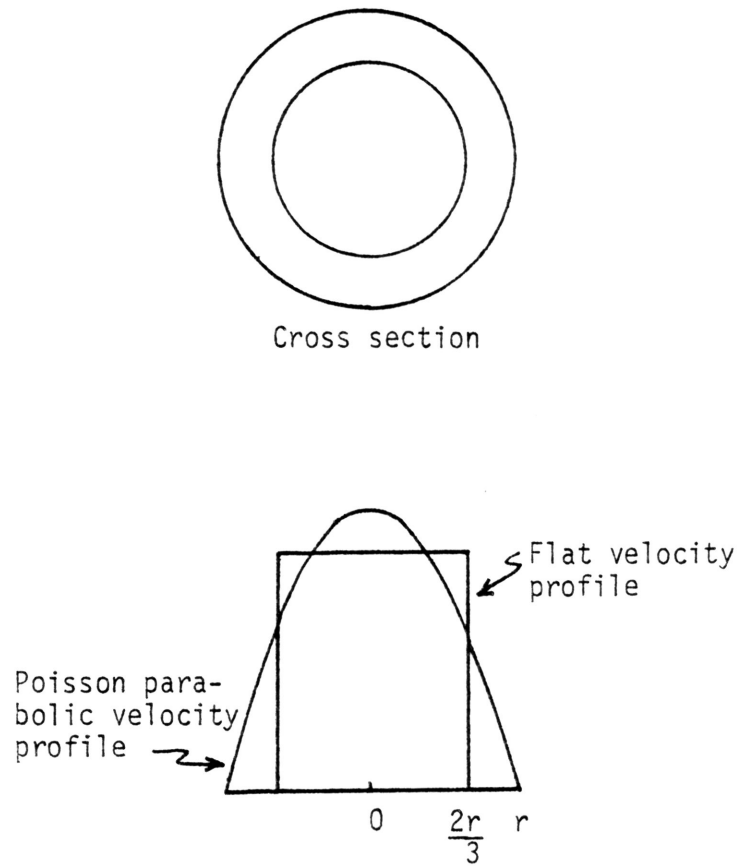


Fig. 8. Flat velocity profile approximation for circular cross section (12).

Rewriting equation (16) in difference form yields

$$\Delta P = \frac{9}{4} \frac{\rho \Delta Z}{\pi r^2} \frac{dQ}{dt} \quad (17)$$

The fluid inductance (L) is

$$L = \frac{9}{4} \frac{\rho \Delta Z}{\pi r^2} \quad (18)$$

where $\Delta P = L \frac{dQ}{dt}$

This fluid inductance term is identical to that derived by Rideout and Dick and takes into account the effects of fluid inertia upon flow.

The transverse impedance is, as stated previously, dependent upon the elastic properties of the wall. It is therefore necessary to analyze the effect of pressure on the arterial walls. If a pressure P is applied to a linearly elastic thin wall vessel of thickness h and a radius of curvature r (Fig. 9) then the circumferential stress S is given by the law of Laplace (13) as

$$S = \frac{Pr}{h} \quad (19)$$

This pressure P will also cause displacement of the wall (Fig. 10). If the longitudinal strain is assumed to be negligible, which is a good assumption due to the small strains found in the arteries, then the circumferential stress is given as (14)

$$S = \frac{E \frac{dr}{r}}{(1-\nu^2)} \quad (20)$$

where dr = change in radius of curvature

E = Young's modulus

ν = Poisson's ratio

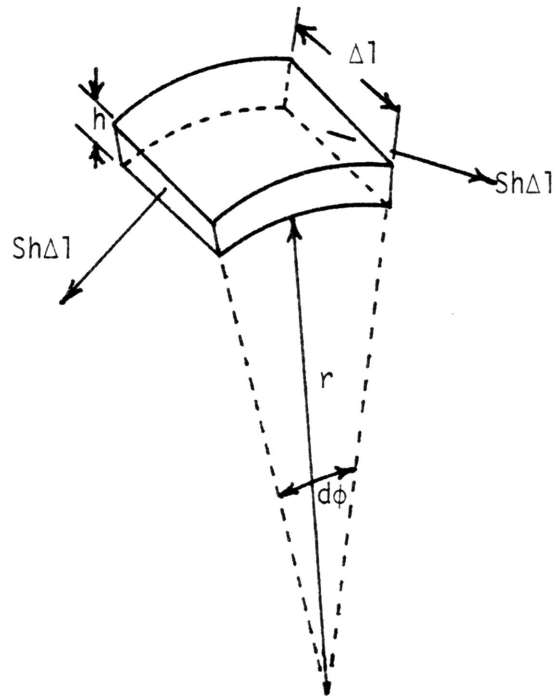


Fig. 9. Segment of a thin walled tube. S = circumferential stress (3).

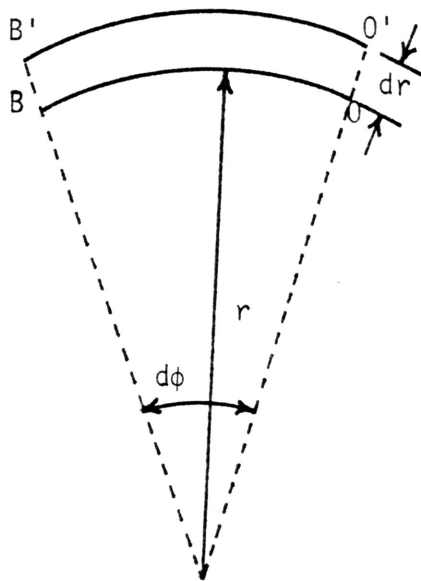


Fig. 10. Radial wall displacement of a thin walled tube (14).

Setting equation (19) equal to equation (20) and solving for dr yields

$$dr = \frac{\Delta P r^2 (1-\nu^2)}{Eh} \quad (21)$$

Also

$$dV = r \, d\phi \, dr \, \Delta z \quad (22)$$

where dV = volume of differential element

$d\phi$ = differential angle

Substituting the expression for dr into dV yields

$$dV = \frac{\Delta P (1-\nu^2) \Delta z}{Eh} r^3 \, d\phi \quad (23)$$

The difference in flow rate in and out of a section of artery can be related to volume changes by

$$dV = \Delta Q \, dt \quad (24)$$

where $\Delta Q = Q_{in} - Q_{out}$

Setting equation (23) equal to equation (24) and integrating yields

$$\int_0^t \Delta Q \, dt = \frac{\Delta P (1-\nu^2) \Delta z}{Eh} \int_0^{2\pi} r^3 \, d\phi \quad (25)$$

The fluid capacitance relating blood flow to the elastic properties of the blood vessel is C where

$$C = \frac{2\pi r^3 \Delta z (1-\nu^2)}{Eh} \quad (26)$$

and $\Delta Q = C \frac{dP}{dt}$

A dumbbell configuration corresponds to two disjoint circular cross sections. The R , L , and C values for each of these circular are identical to those found for a circular cross section.

Elliptical Cross Section Impedance Characteristics

The techniques used to derive the impedance characteristics for the circular cross section are applicable to the elliptical cross section. First, the resistance term is desired. The assumptions are as before. For an elliptical cross section the axial velocity U_z is given as (15)

$$U_z = \frac{1}{2\mu} \frac{dP}{dz} \frac{a^2 b^2}{a^2 + b^2} \left(1 - \left(\frac{x^2}{a^2} + \frac{y^2}{b^2} \right) \right)$$

where μ = viscosity

P = pressure

z = axial distance

a = minor axis length

b = major axis length

The volumetric flow rate (Q) is given as (15)

$$Q = \frac{\pi}{4\mu} \frac{dP}{dz} \frac{a^3 b^3}{a^2 + b^2} \quad (27)$$

Rewriting equation (27) in difference form and solving for ΔP yields

$$\Delta P = \frac{4\mu \Delta z (a^2 + b^2)}{\pi a^3 b^3} Q$$

For an elliptical cross section the resistance term (R) is given

as

$$R = \frac{4\mu \Delta z (a^2 + b^2)}{\pi a^3 b^3} \quad (28)$$

where $\Delta P = RQ$

The difference for the elliptical cross section inductance term arises as a result of the equation

$$Q = \frac{1}{\rho} \frac{dP}{dz} \iint_A dA \quad (29)$$

A flat velocity profile is once again assumed (Fig. 11). The velocity falls off to zero on the major axis at $A = \frac{2a}{3}$ and on the minor axis at $B = \frac{2b}{3}$. Evaluating equation (29) over this cross sectional area yields

$$Q = \frac{4}{9} \frac{ab}{\rho} \frac{dP}{dz} \int dt \quad (30)$$

Manipulating equation (30) in the same manner as equation (15) yields the inductance term for an elliptical cross section

$$L = \frac{9}{4} \frac{\rho \Delta z}{\pi ab} \quad (31)$$

The difference in the derivation for an elliptical capacitance occurs at equation (25)

$$\int_0^t \Delta Q dt = \frac{\Delta P (1-v^2) \Delta z}{Eh} \int_0^{2\pi} r^3 d\phi \quad (25)$$

For an ellipse the radius of curvature (r) is dependent upon ϕ and is given as (13)

$$r = \frac{a^2 b^2}{(a^2 \sin^2 \phi + b^2 \cos^2 \phi)^{3/2}}$$

The manipulation of equation (25) is the same for the elliptical cross section as the circular cross section. The capacitance (C) is given as

$$C = \frac{\Delta z (1-v^2)}{Eh} \int_0^{2\pi} r^3 d\phi \quad (32)$$

where r = radius of curvature of an ellipse

$$\text{and } \Delta Q = C \frac{dP}{dt}$$

The values for R , L , and C for both circular and elliptical cross section are compiled in Table 1. One test of the validity of the ex-

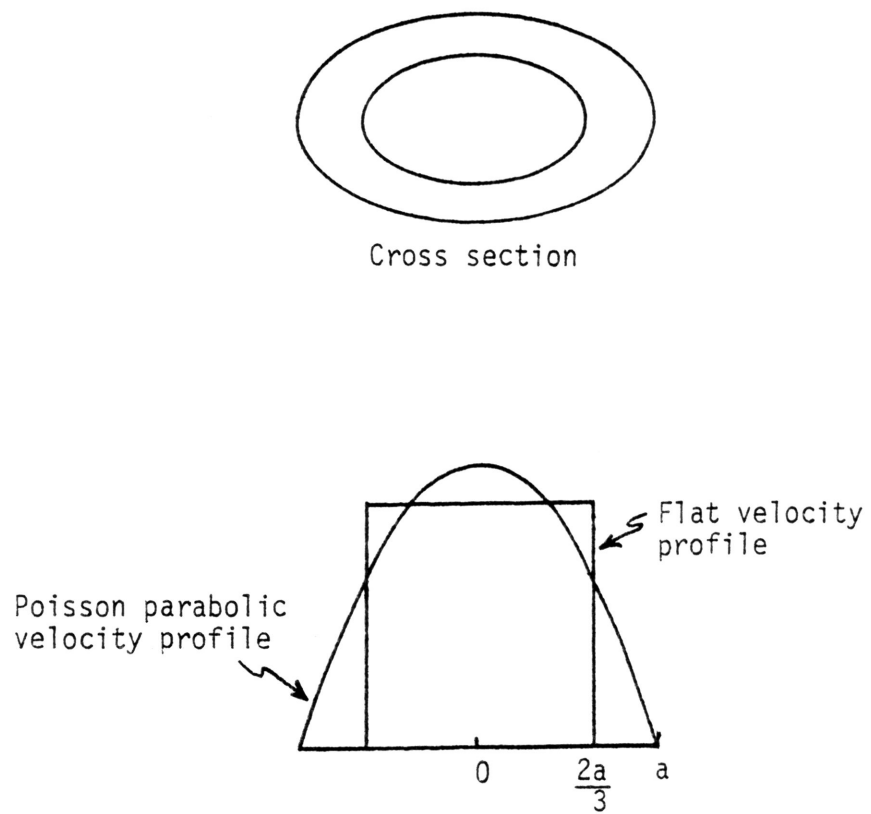


Fig. 11. Flat velocity profile approximation for elliptical cross section.

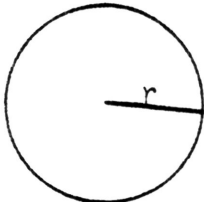
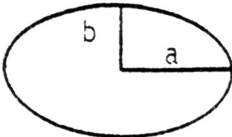
		
R	$\frac{8\mu\Delta z}{\pi r^4}$	$\frac{4\mu\Delta z(a^2 + b^2)}{\pi a^3 b^3}$
L	$\frac{9\rho\Delta z}{4\pi r^2}$	$\frac{9\rho\Delta z}{4\pi ab}$
C	$\frac{\Delta z(1-\nu^2)2\pi r^3}{Eh}$	$\frac{\Delta z(1-\nu^2)}{Eh} \int_0^{2\pi} r^3 d\phi$

Table 1. Values of R, L, C for circular and elliptical cross section.

pressions for the elliptical cross section is to notice that the elliptical expressions reduce to the corresponding circular expressions when $a = b = r$. This is the condition corresponding to the evolution of an ellipse into a circle.

Concept of the Fluid/Electrical Analog

The model of the coronary circulation developed herein is based on the derivation of a fluid/electrical analog. The concept behind a fluid/electrical analog is simple: there are certain characteristics of a fluid system which allow it to be expressed in the form of an electrical circuit. This technique allows for conceptual advantages since it becomes a simple matter to apply circuit analysis techniques to the analog circuit. The analogs between the fluid and electrical system are illustrated in Table 2.

If the expressions for resistance, capacitance, and inductance for the fluid system are known, then a set of analogous equations relating pressure and flow can be derived. For an electrical system these equations are

$$\begin{aligned} V &= IR && \text{a)} \\ V &= L \frac{dI}{dt} && \text{b)} \quad (33) \\ I &= C \frac{dV}{dt} && \text{c)} \end{aligned}$$

where V = voltage drop

I = current

t = time

R = resistance

ELECTRICAL SYSTEM	FLUID SYSTEM
Voltage	Pressure
Current	Flow rate
Resistance	Energy loss due to friction.
Inductance	Energy stored due to fluid momentum.
Capacitance	Energy stored due to elastic properties of vessel wall.

Table 2. Fluid and electrical analogs.

L = inductance

C = capacitance

Using the fluid analogs these equations are transformed into the following set of equations:

$$\Delta P = QR \quad \text{a)}$$

$$\Delta P = L \frac{dQ}{dt} \quad \text{b) (34)}$$

$$Q = C \frac{d\Delta P}{dt} \quad \text{c)}$$

where ΔP = pressure drop

Q = mass flow rate

t = time

R = fluid resistance

L = fluid inductance

C = fluid capacitance

Model Configuration

A section of artery was modelled by Rideout and Dick using an L network lumped equivalent form (Fig. 12). The electrical analog has the resistance and inductance terms in series. This is because both of these terms have the effect of creating drops in pressure because of flow through them. The capacitance term is across the pressure into the next section. This is a consequence of equation (24) which shows that volume changes are related to differences in the flow into and out of a section. Placing the capacitance term in an across position allows the capacitance to add to or subtract from the section flow rate. Thus the fluctuations in volume due

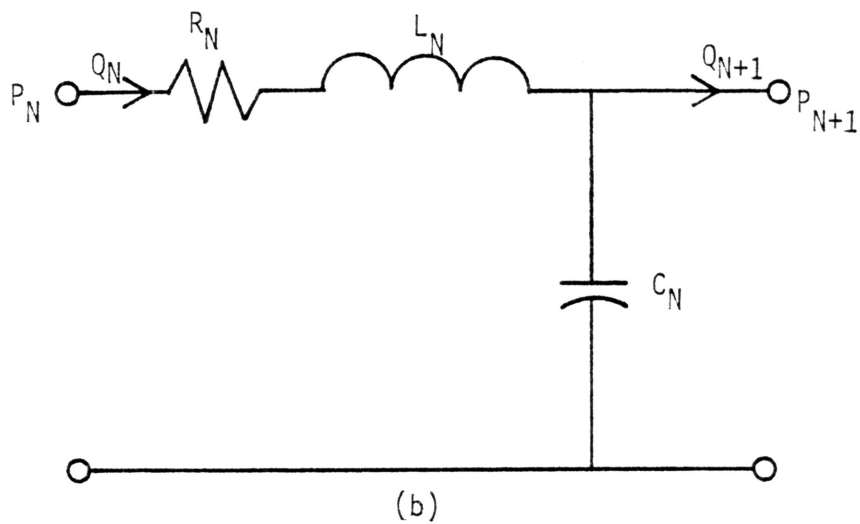
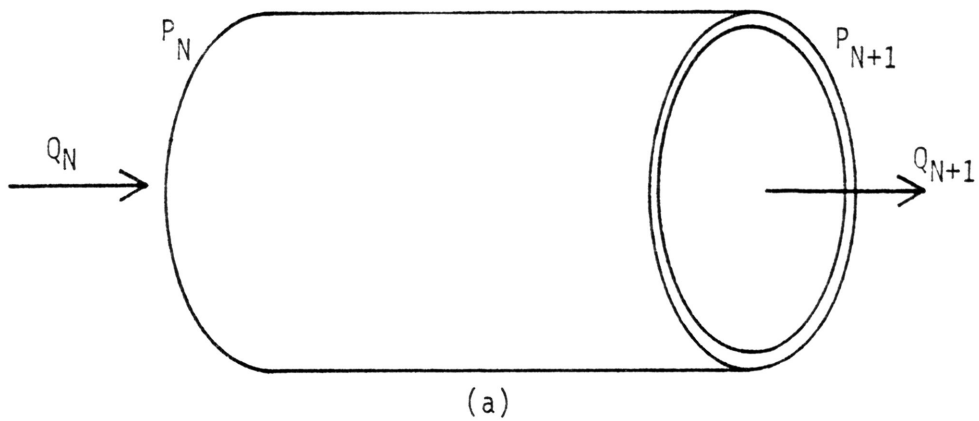


Fig. 12. (a) Section of artery. (b) L network lumped equivalent circuit (12).

to flow rate changes are due to the capacitance term which depends entirely upon the elastic properties of the arterial wall. This arrangement of R, L, and C corresponds to that described by Attinger and Attinger (11) where R and L are the longitudinal impedance terms and C is the transverse impedance term.

For the model of the coronary circulation developed herein, the electrical analog shown in Fig. 13 was proposed. A unique feature of this model is the use of a pressure source (P_{ext}) to represent the pressure developed in the myocardium during the cardiac cycle. The validity of this sectional representation can be visualized by comparing the response of the electrical section to the response of the arterial section. If a step input of external pressure is applied to both systems there will be a transient flow of liquid in the fluid section and a corresponding transient current in the electrical section. Also, if the vessel walls should become rigid the effects of external pressure becomes less. Similarly, for the electrical section, a rigid wall will have a large Young's modulus which corresponds to a decreasing capacitance and a lessening of the effects of external pressure (P_{ext}).

The system developed by Rideout and Dick was entirely linear. However, this model allows for variations in cross sectional shape which is determined from changes in section volume. Since section volume change (dV) is related to difference in flow rate in and out of a section ΔQ by

$$dV = \Delta Q dt$$

and change in volume is also

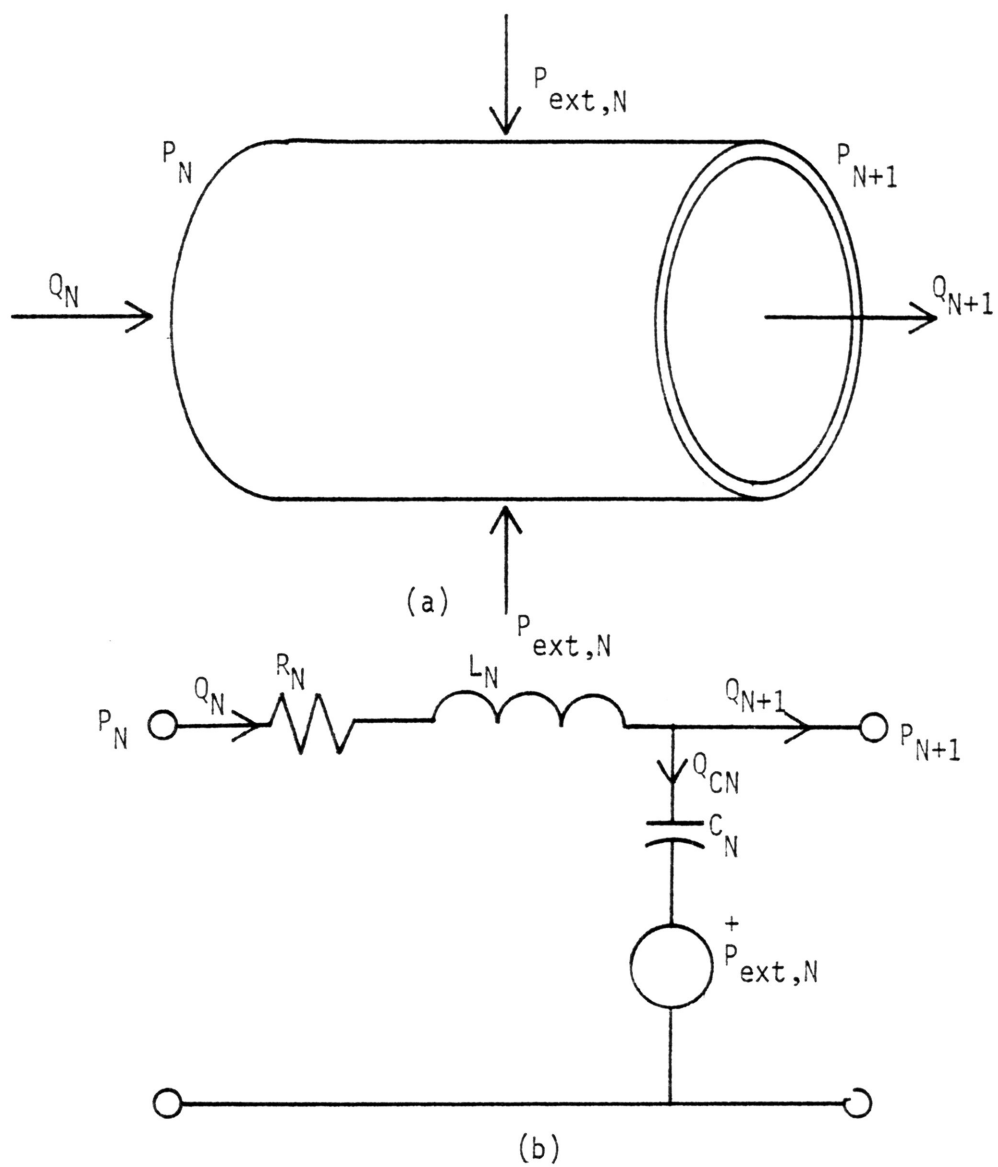


Fig. 13. (a) Section of coronary artery. (b) L network lumped equivalent circuit.

$$dV = dA dz$$

Therefore, the change in cross section area (dA) is given by

$$dA = \Delta Q \frac{dt}{dz}$$

The change in cross sectional area can be used to determine the new cross sectional area for the next time interval. Similarly, the new cross sectional configuration can be determined using the previously mentioned cut off ratios. From the new cross sectional configuration and area the new values of R , L , and C can be determined. Examination of Table 1 shows R , L , and C to be sensitive functions of cross sectional area and configuration. Therefore, the model becomes highly nonlinear over several intervals.

III. METHODS

Derivation of Controlling Equations

The derivation of the controlling equations for a coronary arterial section (Fig. 13) are based upon state-variable analysis. The subscript N identifies the section. The subscript T identifies the period in time.

The first equation necessary is an expression for the inlet flow $Q_{N,T}$. Summing pressures yields

$$P_{N,T} - R_N Q_{N,T} - L_N \frac{dQ_{N,T}}{dt} - P_{N+1,T} = 0 \quad (35)$$

Rewriting equation (35) in terms of $Q_{N,T}$ yields

$$\frac{dQ_{N,T}}{dt} = \frac{1}{L_N} (P_{N,T} - R_N Q_{N,T} - P_{N+1,T}) \quad (36)$$

The final equation necessary is an expression for the outlet pressure $P_{N+1,T}$. The flow through the capacitor $Q_{CN,T}$ is given as

$$Q_{CN,T} = Q_{N,T} - Q_{N+1,T} \quad (37)$$

Writing the flow through the capacitor in terms of the pressure across the capacitor ($P_{CN,T}$) yields

$$C_N \frac{dP_{CN,T}}{dt} = Q_{N,T} - Q_{N+1,T} \quad (38)$$

The pressure across the capacitor may be written in terms of the external pressure ($P_{EN,T}$) and outlet pressure ($P_{N+1,T}$)

$$P_{CN,T} = P_{N+1,T} - P_{EN,T} \quad (39)$$

Substituting equation (39) into equation (38) and rearranging for

an expression in terms of $P_{N+1,T}$ yields

$$\frac{dP_{N+1,T}}{dt} = \frac{1}{C_N} (Q_{N,T} - Q_{N+1,T}) + \frac{dP_{EN}}{dt} \quad (40)$$

The derivation is similar for the dumbell configuration. In this case the circuit is as shown in Fig. 14. For this analog circuit the controlling equations are

$$\frac{d \frac{Q_{N,T}}{2}}{dt} = \frac{1}{L_N} (P_{N,T} - R_N \frac{Q_{N,T}}{2} - P_{N+1,T}) \quad (41)$$

$$\frac{dP_{N+1,T}}{dt} = \frac{1}{C_N} \left(\frac{Q_{N,T}}{2} - \frac{Q_{N+1,T}}{2} \right) + \frac{dP_{EN}}{dt} \quad (42)$$

Implementation of equations (36), (40), (41), and (42) on a digital computer is necessary. This requires that these equations be written in finite divided difference form. Assuming that the pressure and flows are to be calculated over some interval (T_1, T_2) and that the length of the interval is ΔT yields two sets of approximating equations.

For the elliptical or circular cross section these are

$$Q_{N,T_2} = \frac{1}{L_N} (P_{N,T_1} - R_N Q_{N,T_1} - P_{N+1,T_1}) \Delta T + Q_{N,T_1} \quad (43)$$

$$P_{N+1,T_2} = \frac{1}{C_N} (Q_{N,T_1} - Q_{N+1,T_1}) \Delta T + P_{EN,T_2} - P_{EN,T_1} + P_{N+1,T_1} \quad (44)$$

For the dumbell cross section these are

$$Q_{N,T_2} = \frac{2}{L_N} (P_{N,T_1} - R_N \frac{Q_{N,T_1}}{2} - P_{N+1,T_1}) \Delta T + Q_{N,T_1} \quad (45)$$

$$P_{N+1,T_2} = \frac{1}{2C_N} (Q_{N,T_1} - Q_{N+1,T_1}) \Delta T + P_{EN,T_2} - P_{EN,T_1} + P_{N+1,T_1} \quad (46)$$

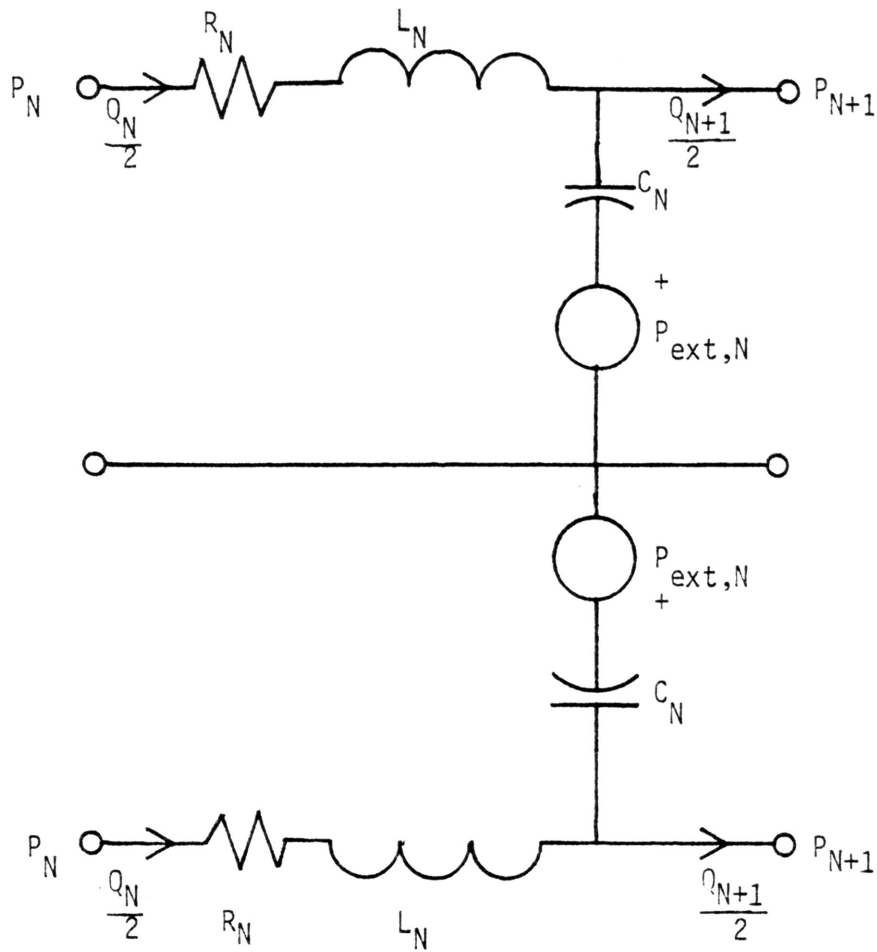


Fig. 14. L network lumped equivalent circuit for a dumbbell cross section.

Equations (43-46) constitute a recursion relationship for calculating pressures and flows in a section of coronary artery. Several sections of artery may be connected in series and pressure and flow in each section computed. A generalized flow chart illustrating the implementation of equations (43-46) and the change in cross sectional configuration is shown in Fig. 15. An explanation of the subroutines involved and a complete program listing are located in the appendix.

Description of Model Experiments

The implementation of the model of flow through a coronary vessel required that several parameters describing the arterial vessel be chosen. The choice of these parameters was based on previous discussions. The value of Young's modulus was 5×10^6 dyne/cm². Assuming the arterial wall to be incompressible, Poisson's ratio is $\frac{1}{2}$. The vessel wall thickness was 0.0096 cm. The vessel radius was 0.048 cm. The viscosity of blood used was 0.03 poise and the density of blood used was 1.05 g/cm³. Three sections with a length of 4 cm/section were connected in series. This series representation of a coronary arterial segment is illustrated in Fig. 16.

The final assumption made concerned the representation of the pressure developed in the myocardium during ventricular contraction. There are, as noted previously, great difficulties involved in the analysis of myocardial stress. Since the time course and trends of myocardial stress are essentially similar to those of ventricular

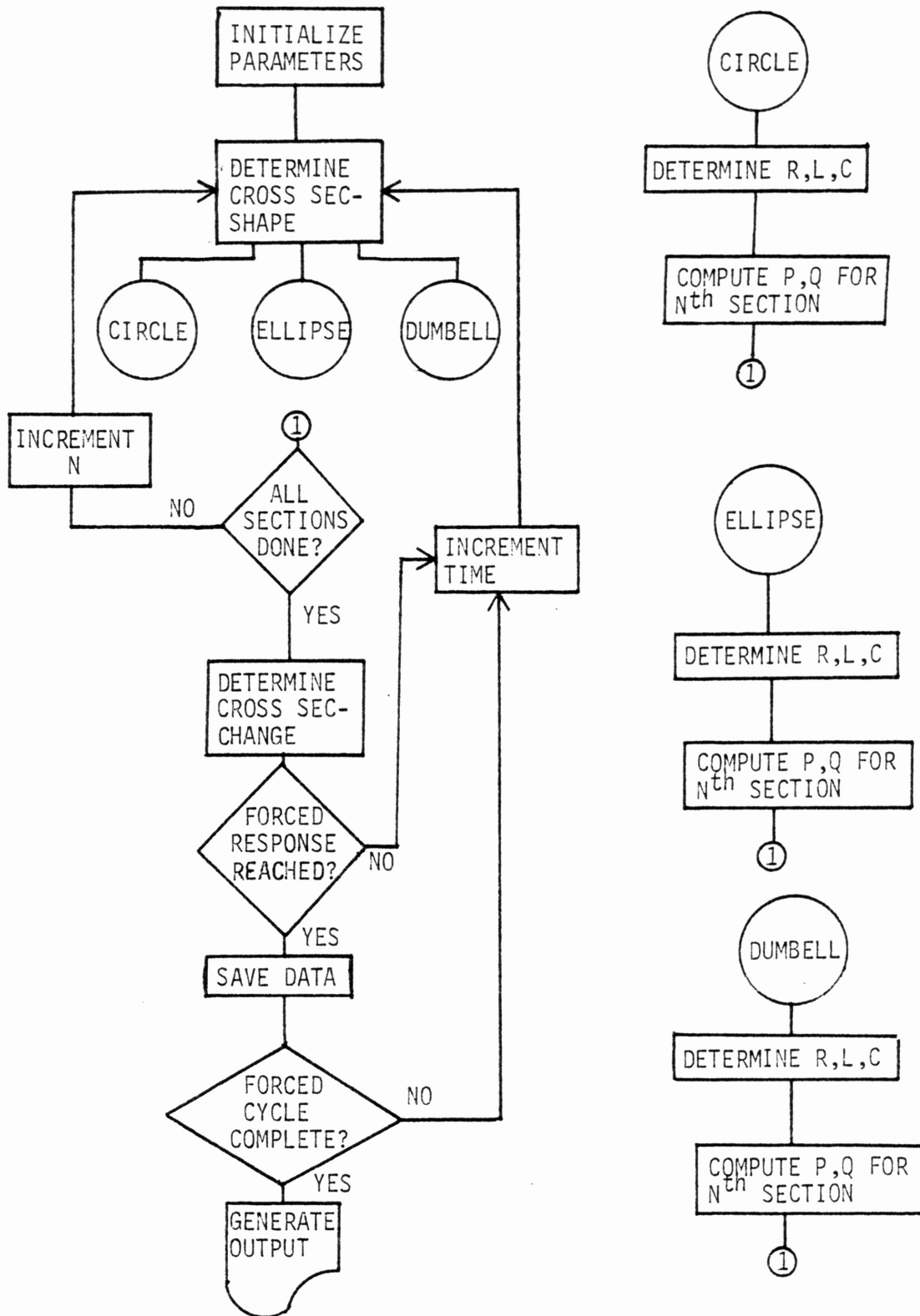


Fig. 15. Generalized flow chart for coronary blood flow model.

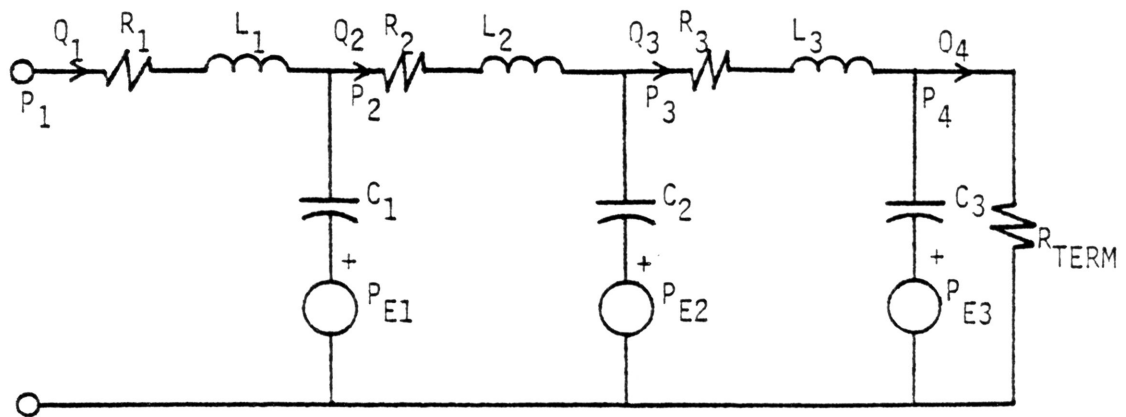


Fig. 16. Implemented model of a coronary arterial segment.

pressure, the ventricular pressure waveform was used to represent the myocardial pressure. The aortic pressure was used as a driving pressure for the system. The aortic and ventricular pressures used in the model are shown in Fig. 17.

An analysis of the general relationship between the R, L, and C parameters and cross sectional area was performed. The first model developed modelled the effects of simultaneous ventricular contraction on a coronary vessel. The second model was an attempt to more accurately describe the actual contraction mechanism of the left ventricle. The second model modelled the effects of a ventricular contraction beginning at the apex of the heart and propagating upward.

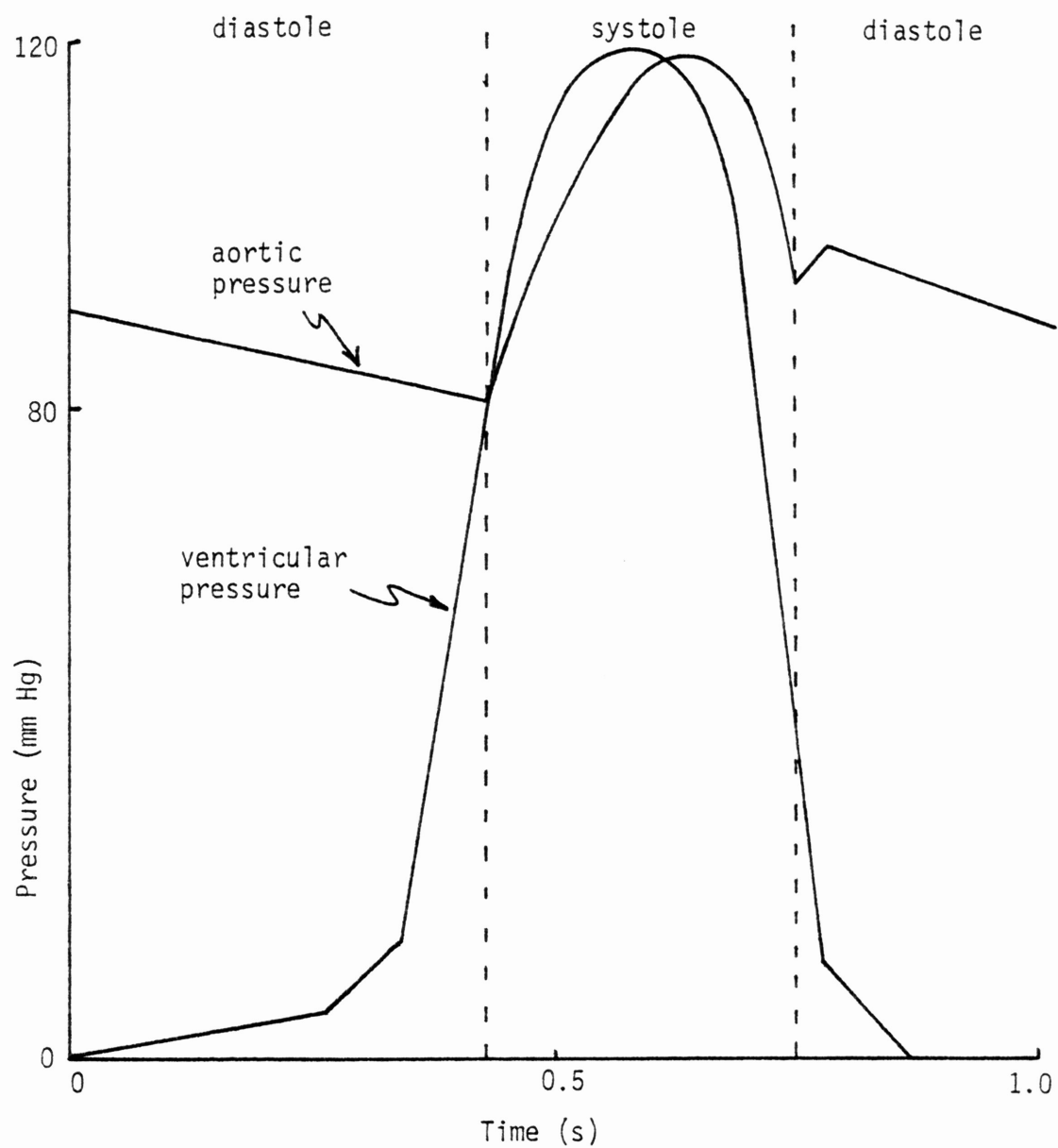


Fig. 17. Aortic and ventricular pressure waveforms.

IV. RESULTS

Before the implementation of the model of the coronary circulation, an analysis of the impedance terms was performed. The general trends for the R, L, C and parameters as a function of cross sectional area are shown in Fig. 18. The resistance and inductance terms are inversely proportional to the cross sectional area as expected. The capacitance term exhibits an interesting behavior.

As the elliptical cross section becomes flatter, the capacitance increases. The increasing capacitance for the flatter ellipse is a result of the dependency of the capacitance on the radius of curvature of the ellipse. For a flatter ellipse the radius of curvature increases greatly over a significant portion of the ellipse. Since the capacitance for an ellipse is proportional to $\int r^3 d\phi$, the capacitance increases. This indicates that the ellipse is relatively easily deformed. Once the cross section collapses to a dumbbell configuration, the capacitance drops off drastically. This indicates that the dumbbell cross section is much more difficult to deform. The difference between elliptical and dumbbell cross sectional capacitance can also be considered to be a transition from an unstable state to a stable state.

Two models of coronary blood flow were implemented. The first model assumed simultaneous contraction of the left ventricle, that is, the time course of the external pressure was identical in each section of artery (Fig. 19). The second model took into account the effects of ventricular contraction as it propagates from the apex

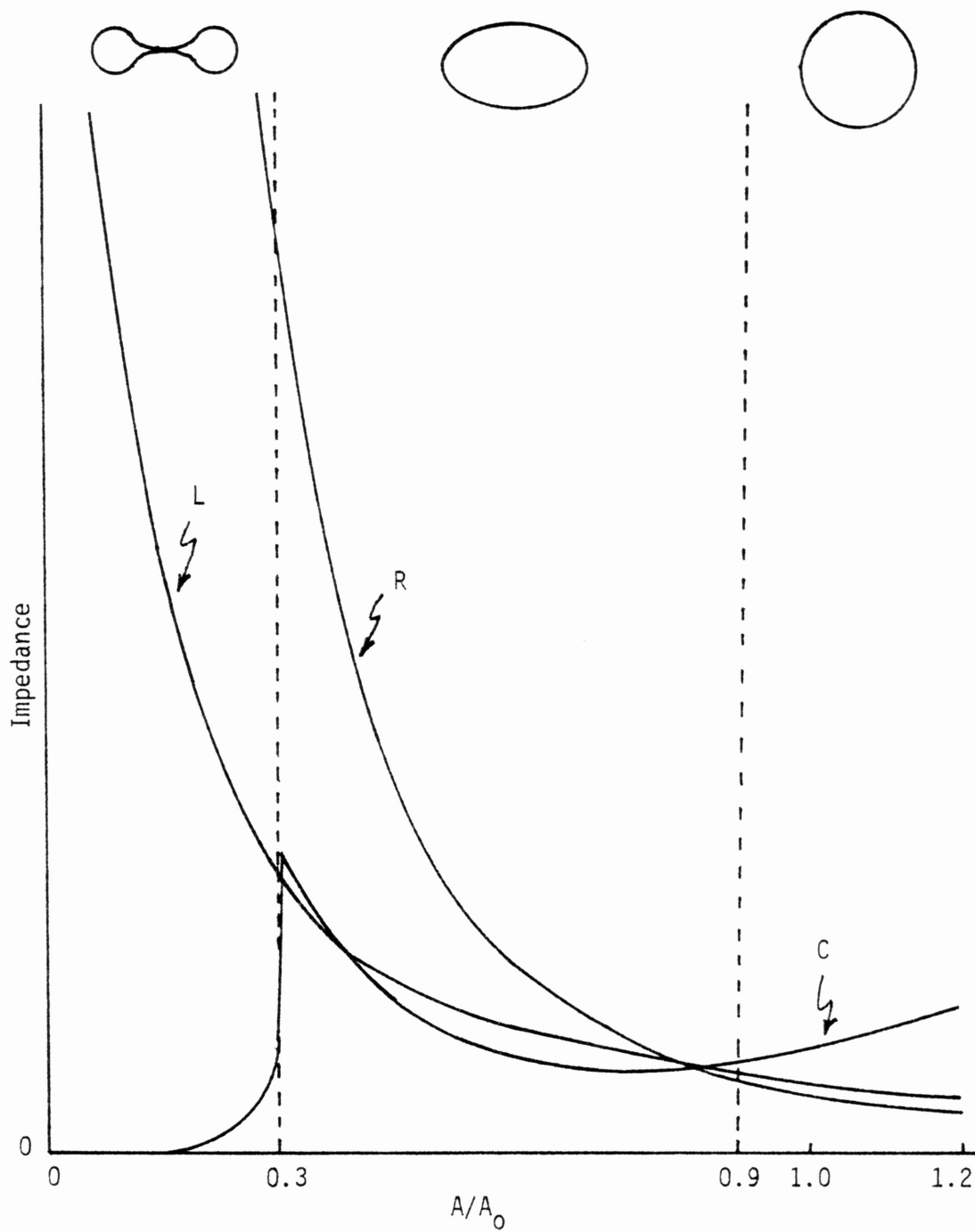


Fig. 18. General trends of R , L , C as a function of area. $A_0 =$ original area.

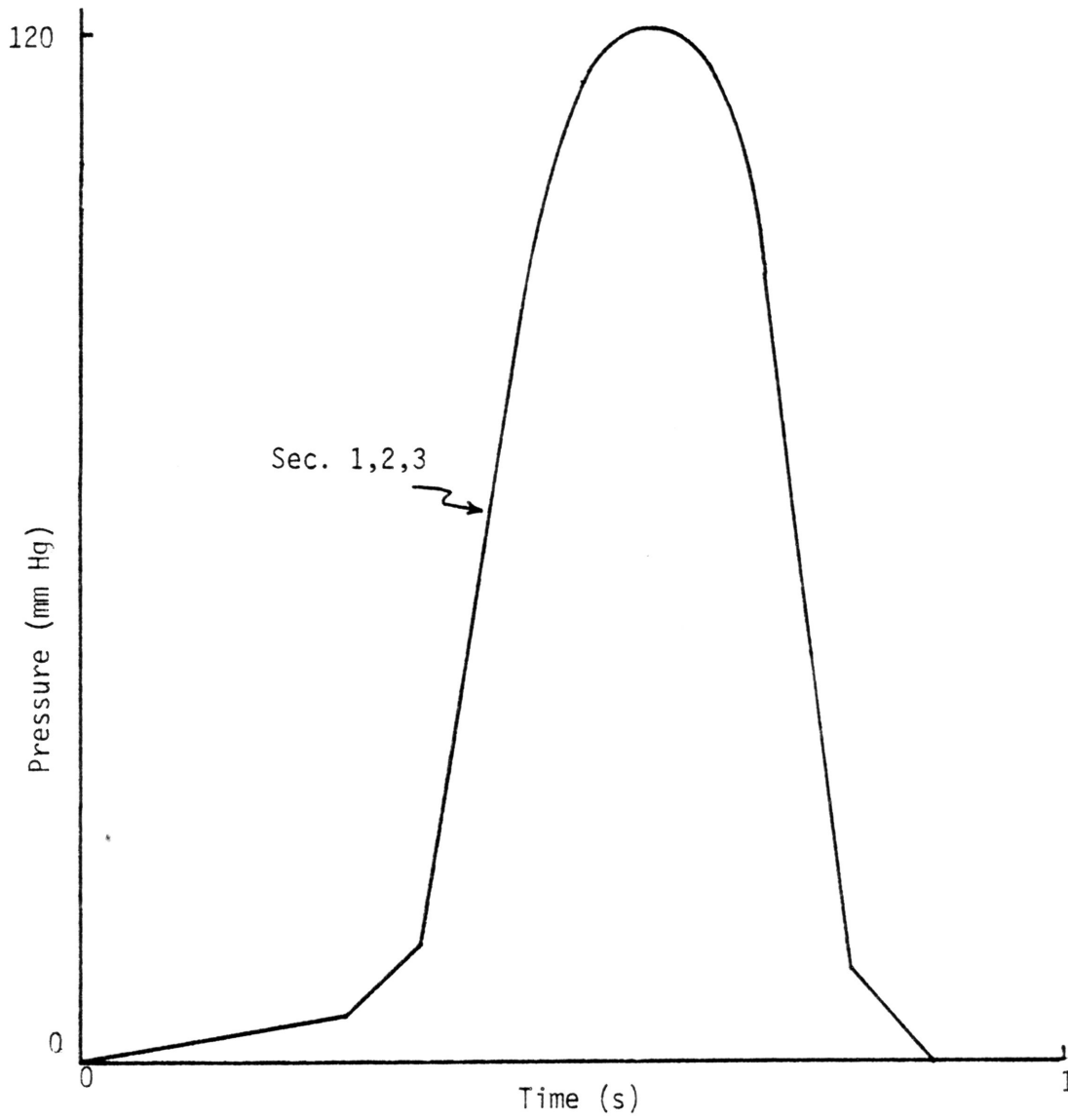


Fig. 19. External pressure in each section for simultaneous contraction.

of the heart to the aortic valve of the left ventricle (Fig. 20). The inclusion of the effects of propagating ventricular contraction is more indicative of the actual situation in the heart.

The first feature of importance in both models is the reaching of the forced response of the system. Fig. 21 shows the contrast between the system's transient flow response due to one heart beat and the forced flow response due to thirty heart beats. The transient curves show the erratic and poorly developed flow curves. The forced response flow curves are in sharp contrast to the transient flow curves. The erratic fluctuations have died out and the flow curves have developed more fully. Running the model through a number of cycles showed that by thirty heart beats the forced response had been reached. Similar results appeared in the cross sectional area curves and the sectional pressure curves.

The pressure, flow, and cross sectional area curves for the first model are shown in Figs. 22, 23, and 24 respectively. The pressure, flow and cross sectional area curves for the second model are shown in Figs. 25, 26, and 27 respectively. Each set of curves for the first and second model has some similar characteristics. The curves will first be considered in terms of general characteristics.

The first curves to be examined are the pressure curves (Figs. 22, 23). The pressure in each section of artery drops the farther from the source that section is. Another interesting aspect of the pressure curves is the degradation of the pressure from the aortic input pressure curve. This is due to the non-linear effects of the

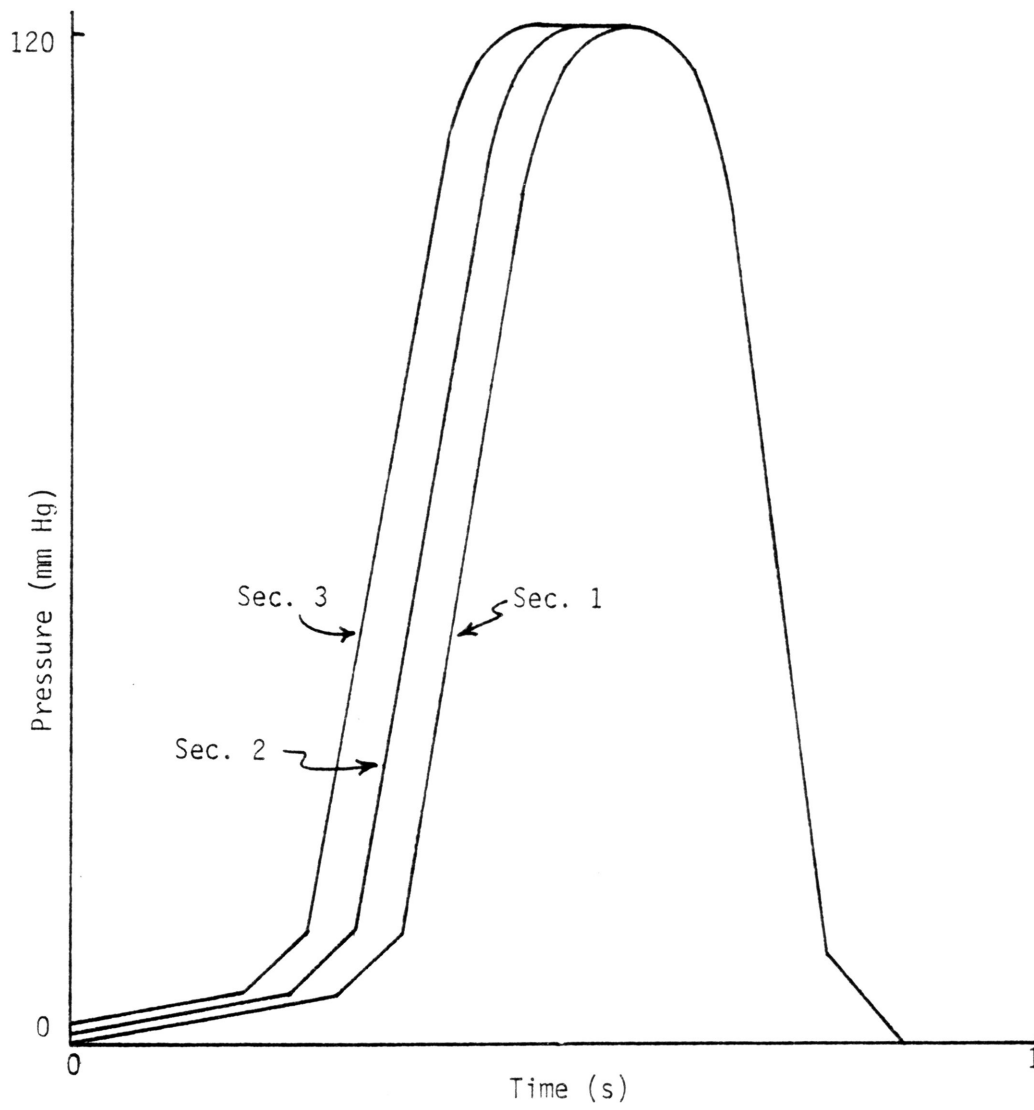


Fig. 20. External pressure in each section for phased contraction.

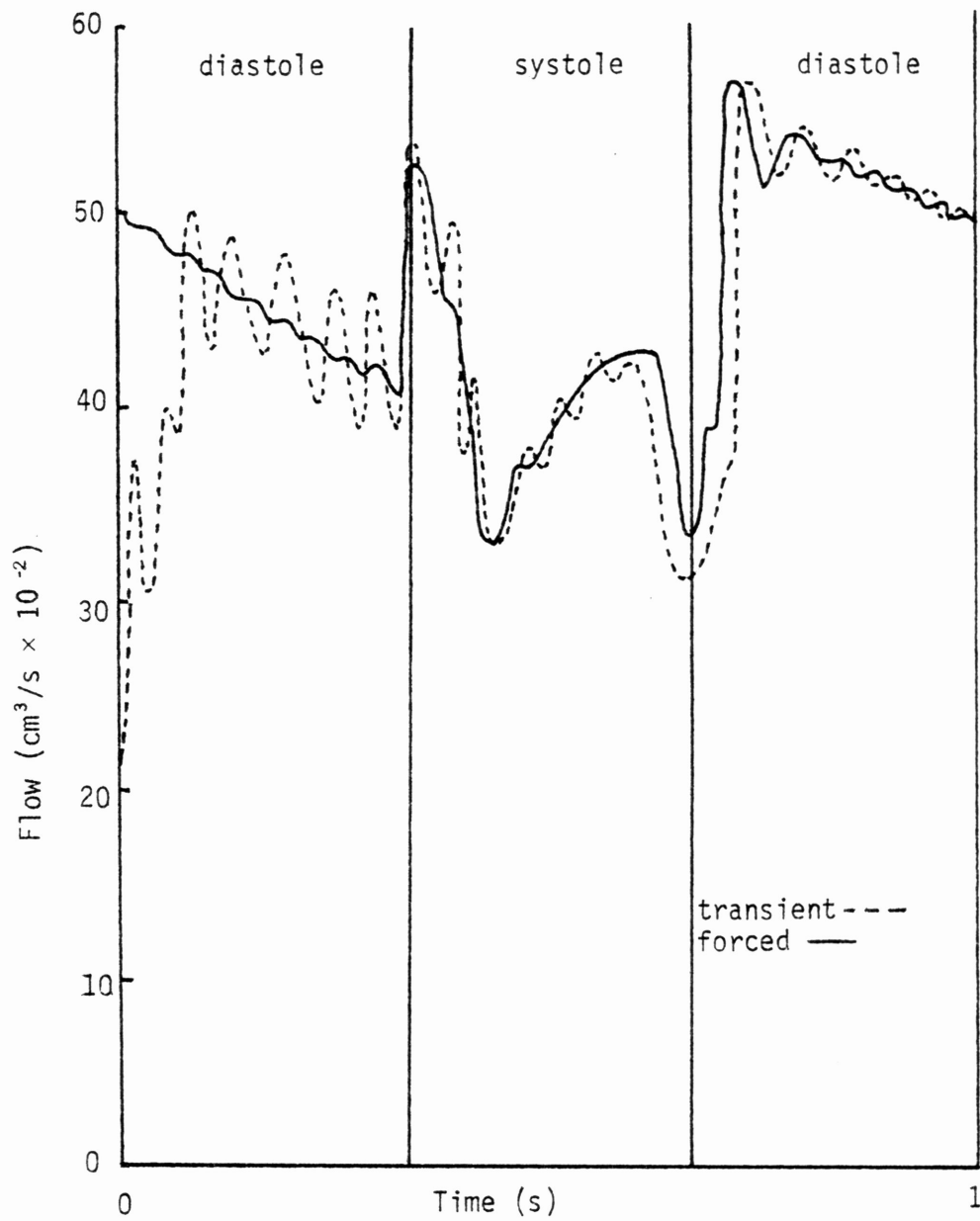


Fig. 21. Transient and forced response flow curves.

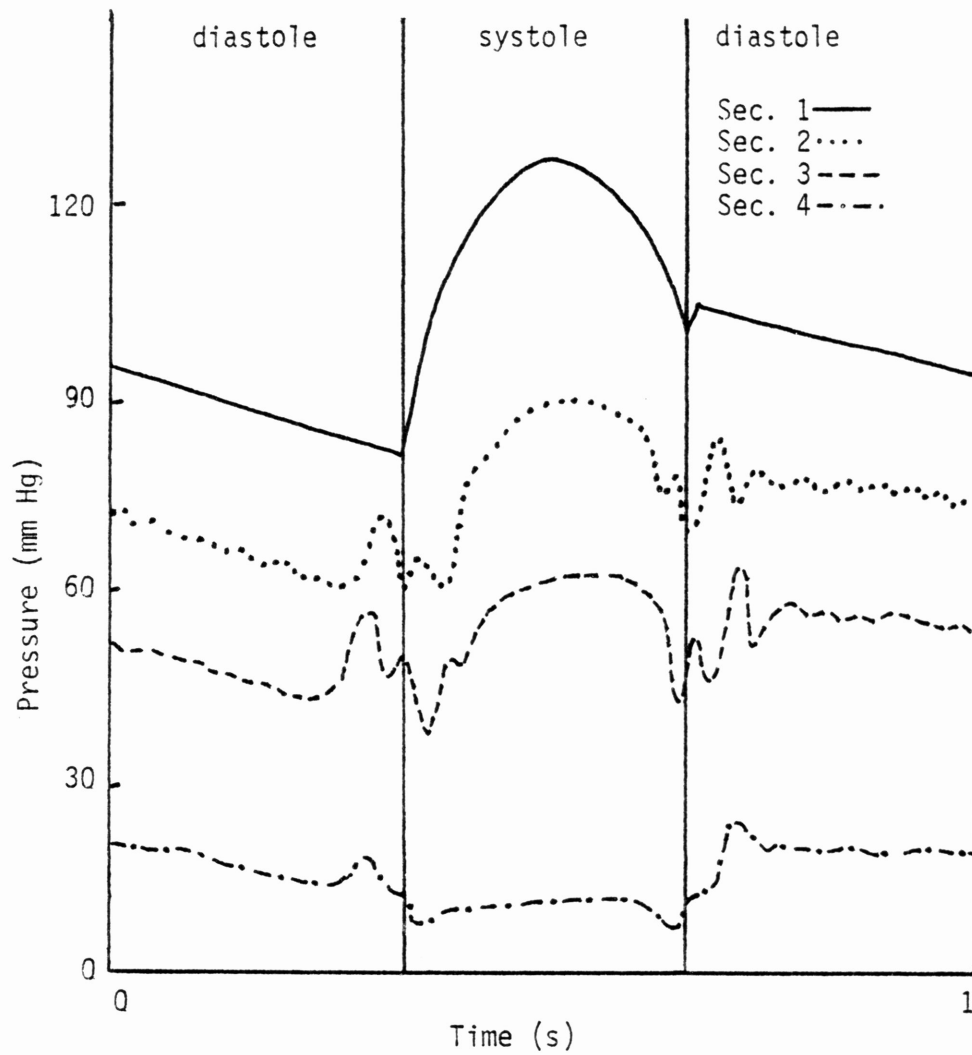


Fig. 22. Sectional pressures for simultaneous ventricular contraction.

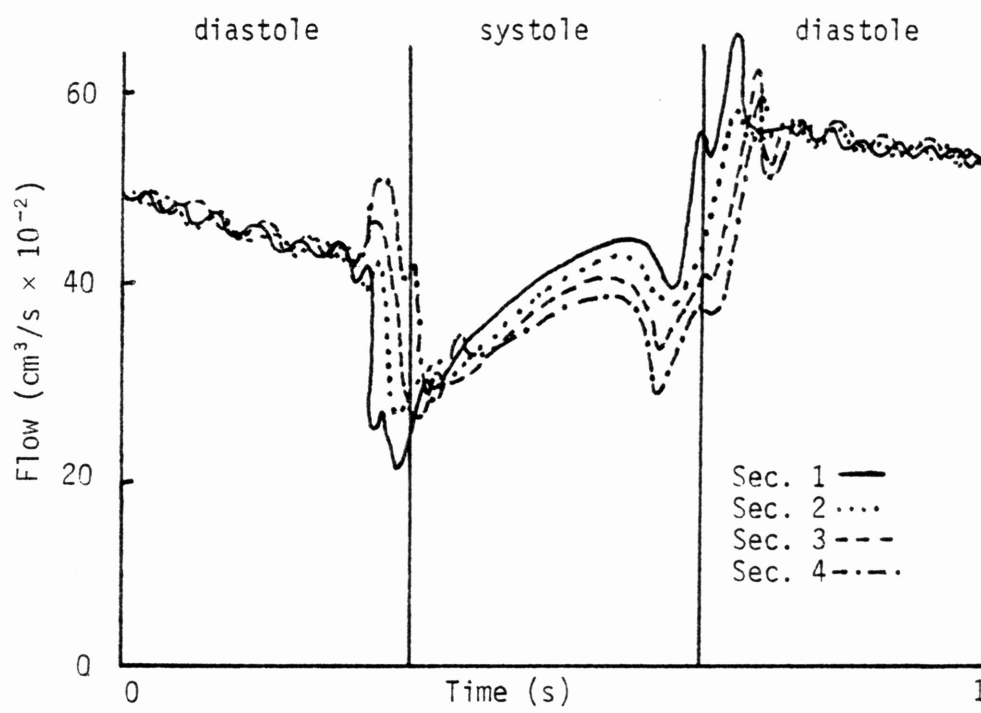


Fig. 23. Sectional flows for simultaneous ventricular contraction.

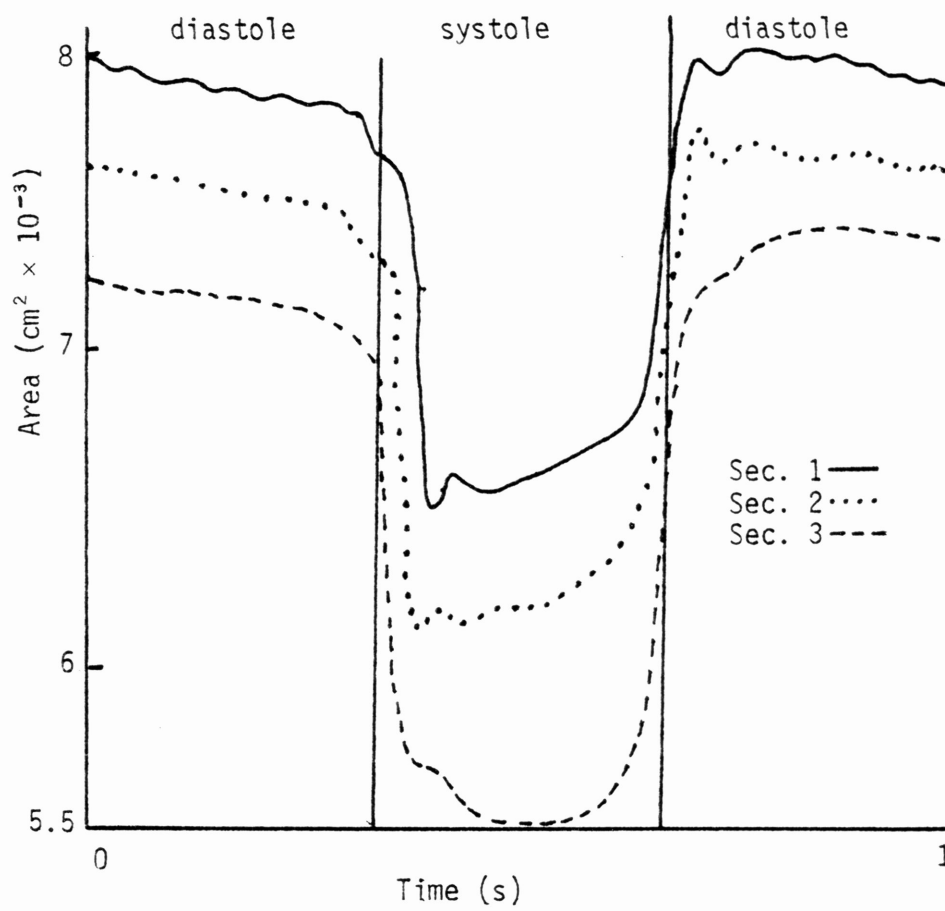


Fig. 24. Sectional areas for simultaneous ventricular contraction.

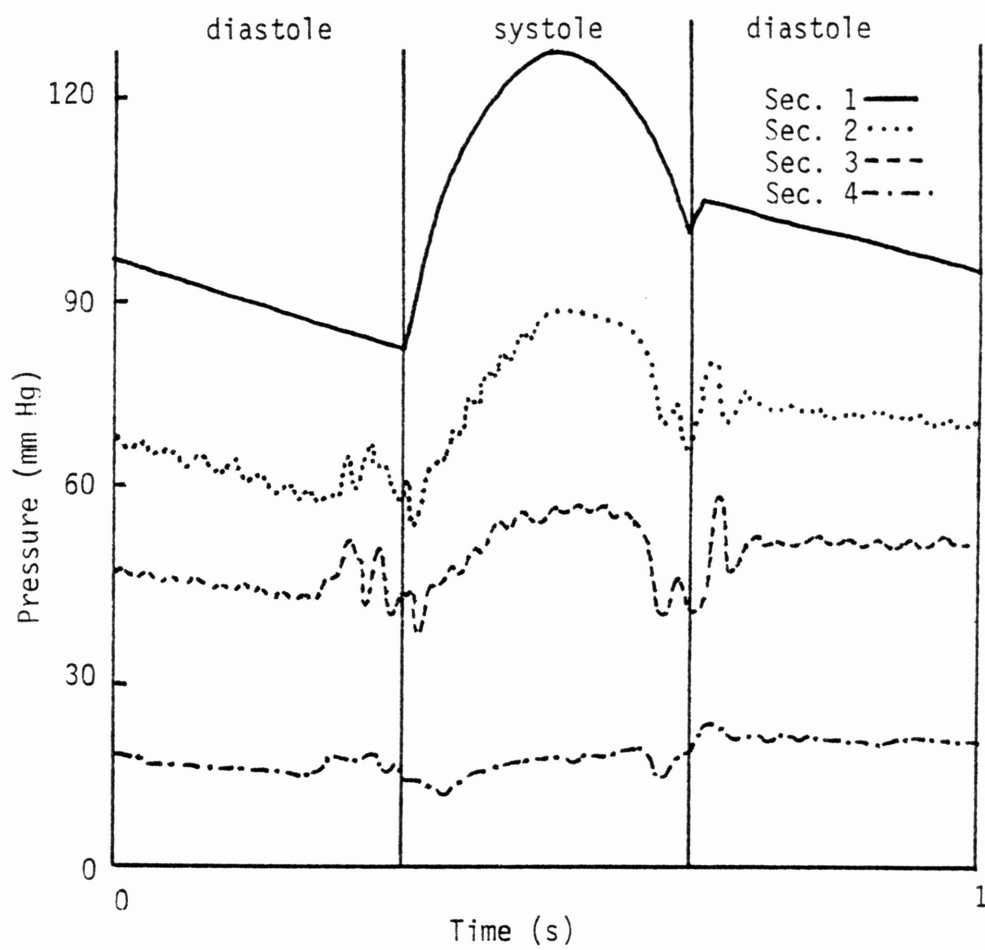


Fig. 25. Sectional pressures for phased ventricular contraction.

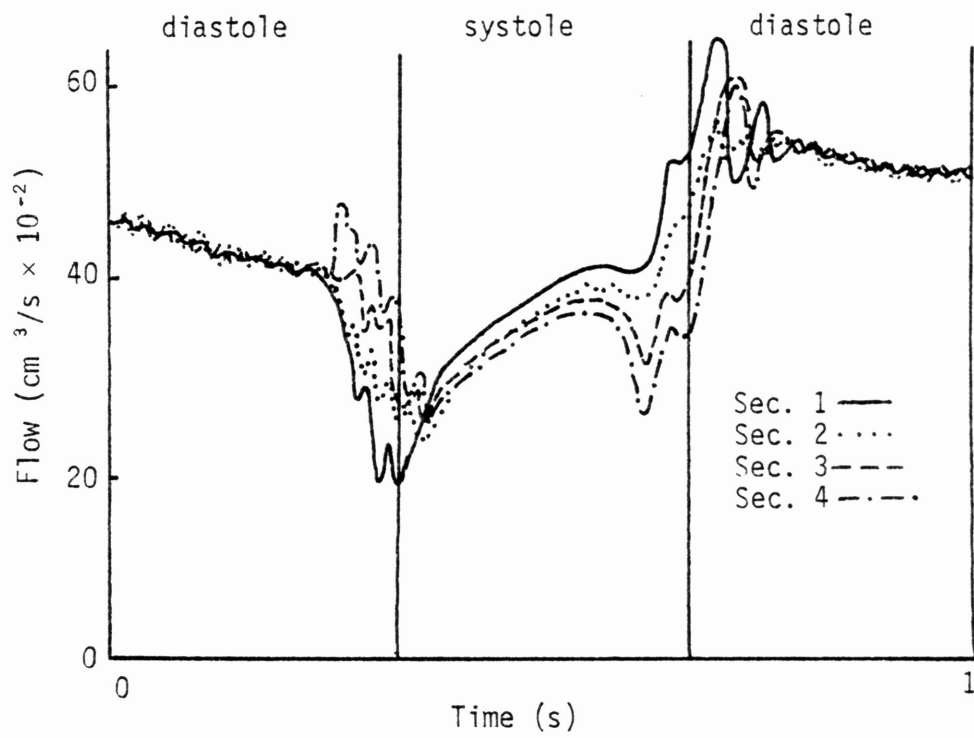


Fig. 26. Sectional flows for phased ventricular contraction.

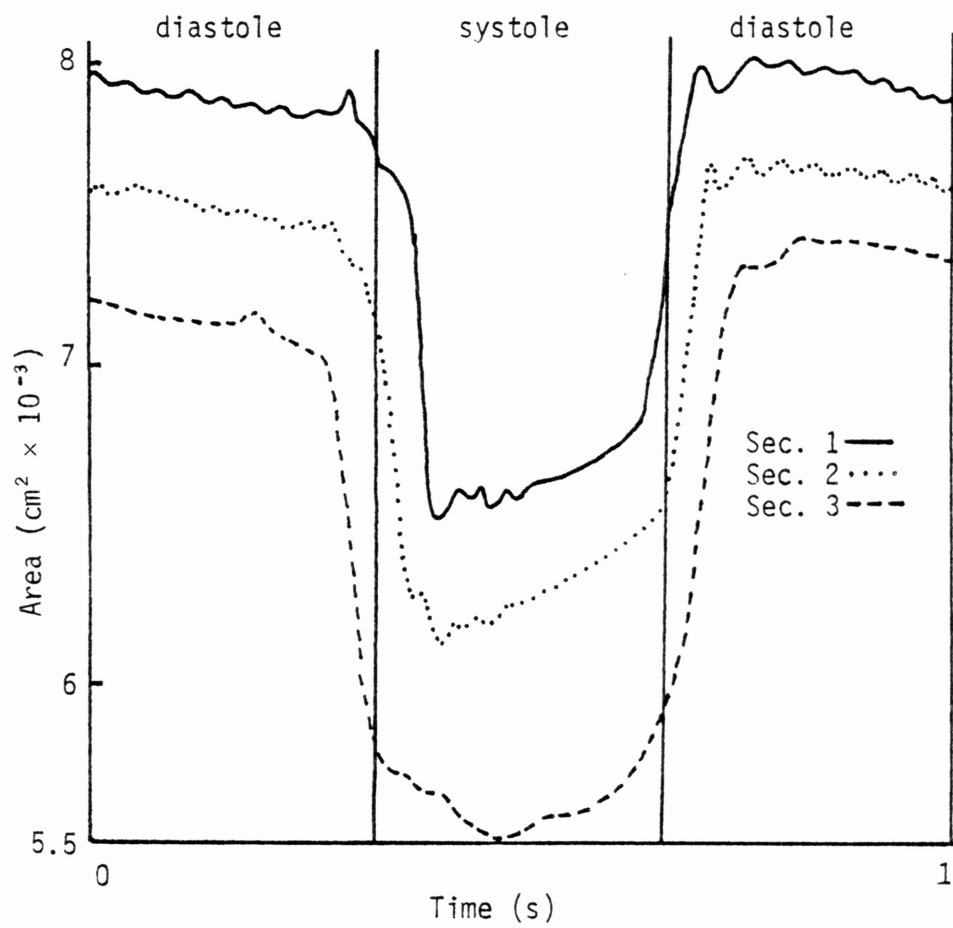


Fig. 27. Sectional areas for phased ventricular contraction.

longitudinal and transverse impedance. The general trend of the sectional pressure curves during diastole is similar to that of the aortic pressure. All of these effects are quite reasonable.

The next curves to be examined in terms of overall characteristics are the flow curves (Figs. 23, 26). Flow generally dropped off in all sections as ventricular contraction began. There is also an increase in flow as the aortic pressure rises sharply and the ventricular pressure begins to level off. The flow follows the aortic pressure during diastole. These general flow characteristics are compatible with measured coronary blood flow characteristics (16).

The final curves to be examined are the cross sectional area curves (Figs. 24, 27). The most noticeable characteristic of these curves is the decrease in cross sectional area as ventricular contraction occurs. The curves are skewed to the left due to the effect of the increasing aortic pressure and the leveling off of the ventricular pressure. It is also interesting to note that the downstream sections undergo a greater collapse. This is because, as noted previously, their internal pressure is correspondingly lower. The lower internal pressure offers less resistance against collapse.

The flow and cross sectional area curves match up quite well. As the cross sectional area decreases due to ventricular contraction, the impedance to flow increases and the flow decreases. The results of the model also seem to indicate that the farther downstream one goes, the less important the arterial pressure is and the more dominant are the effects of ventricular contraction. All of these results are quite reasonable from a cursory viewpoint.

It is also interesting to note the differences between the effects of simultaneous and phased contraction of the left ventricle. The pressure curves are more perturbed during systole for the phased contraction. The pressures are also generally lower for the phased contraction. The phased contraction tends to spread out the flow curves during the first half of systole. The flows are also lower for the phased contraction. The cross sectional area curves are basically the same shape. However, the spreading out of these curves also is seen. All of these effects are due to the phased contraction which has a tendency to spread out its effect through space and time.

Finally, a comparison was made between the general characteristics of the model and measured data. Flow through the coronary arteries has been analyzed by a number of investigators. No applicable pressure curves were found. No measurements of coronary vessel cross sectional area and configuration as a function of aortic and ventricular pressure were found. For these reasons only an analysis of the flows is attempted.

It is important to emphasize that this comparison is made to examine only the general trends in coronary blood flow. The measured flows are flows through major surface vessels which anastomose throughout the myocardium. The model flows are for a vessel running through the myocardium. The assumption is that the general changes in flow and its relationship to aortic pressure should be similar for the model and the measured flow rates. The values of flow shown on the axes pertain only to those generated by the model.

The first flow examined is that through the main left coronary

artery (16). Since it is proximal to the aortic root pressure it will be compared to the first section of the model which is proximal to the aortic pressure source. The results of this comparison for both the phased and simultaneous contraction are shown in Fig. 28. The general characteristics match up well. The flow tends to follow the aortic pressure during diastole in all three cases. There is a rapid drop in flow at the beginning of systole followed by a gradual increase. There is also a sudden increase in flow at the beginning of diastole.

The final flow analyzed was that of the left circumflex coronary arterial flow (16) (Fig. 29). The left circumflex coronary artery is more distal to the aortic root pressure than the main left coronary artery. For this reason, its flow was compared to that in the final section of the modelled coronary artery. Once again, the flow tends to follow the aortic pressure during diastole. There is a general decrease in flow during systole. There is also a sudden increase and decrease at the beginning and end of systole respectively. The results of the comparisons between the model results and the actual flow in the coronary arteries is encouraging.

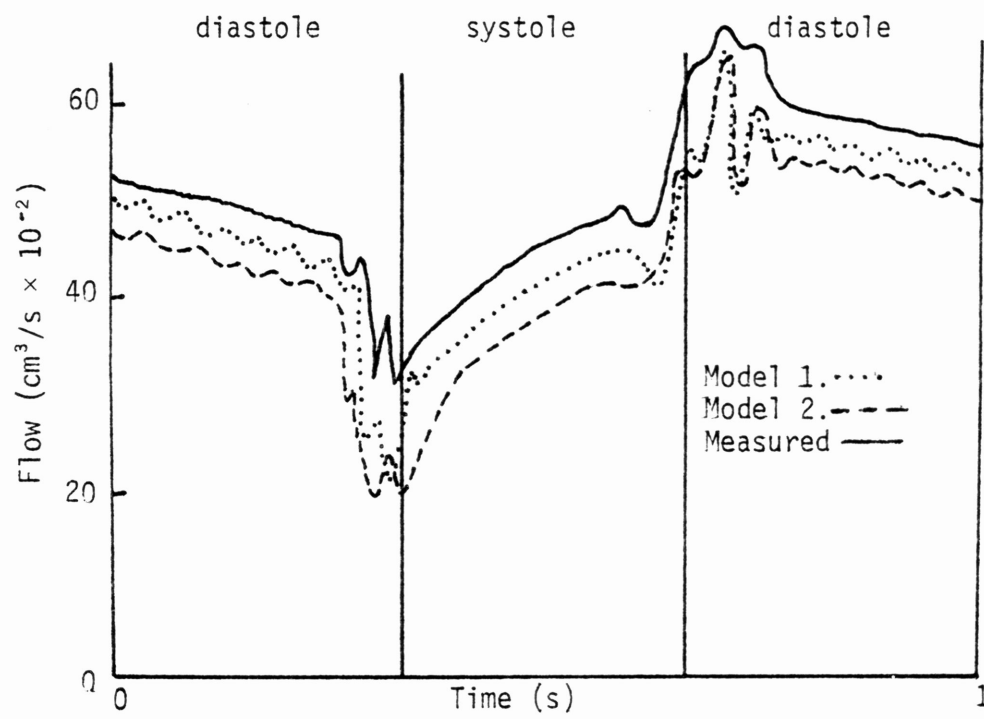


Fig. 28. Modelled and measured flows for the left coronary artery (16).

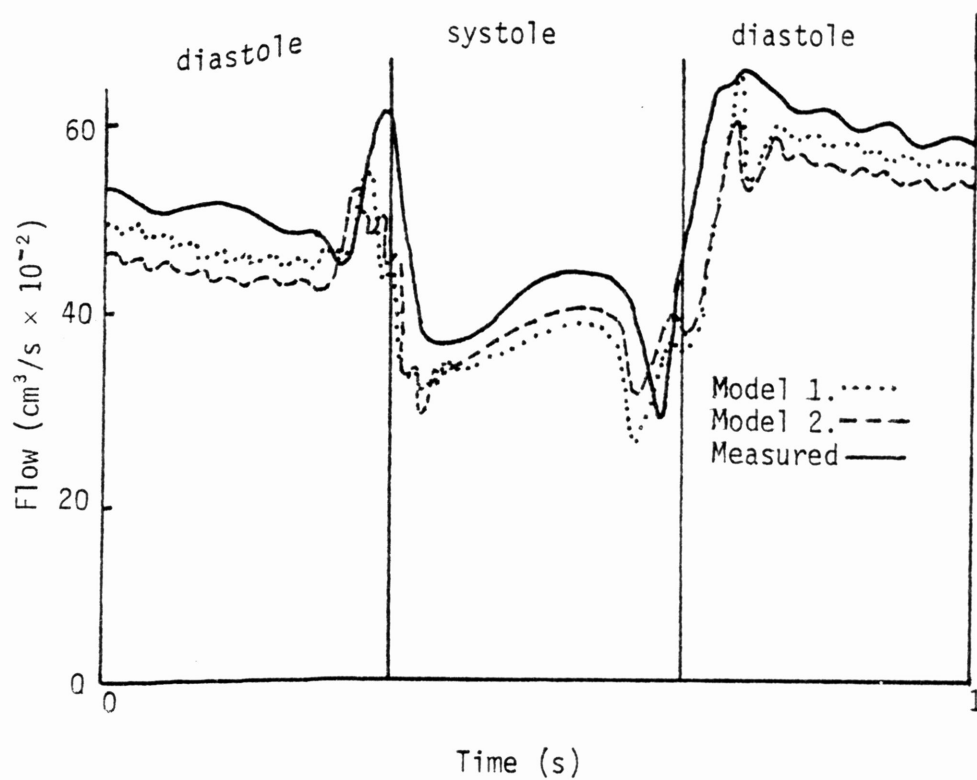


Fig. 29. Modelled and measured flows for the left circumflex coronary artery (16).

V. DISCUSSION

The development of this model was not without some difficulties. The greatest difficulty involved computational time. The time constants associated with this circuit presented some difficulties. By executing the program with the radius used the time constants were set at a reasonable value making a step size of 0.001 seconds possible. The majority of computational time involved the calculations of the elliptical fluid resistance, inductance, and capacitance. This was due to the large number of calculations involved in the integration, root search technique, and circumference determination necessary to calculate the elliptical cross section parameters. The computational time was greatly reduced by calculating the elliptical impedance terms for several cross sectional areas and interpolating the impedance values for other cross sectional areas.

Further validation of this model is necessary. Validation of a model of the coronary circulation would require accurate simultaneous measurements of aortic pressure, myocardial pressure, and coronary blood flow and pressure in a laboratory animal. The model could incorporate a detailed network of vessels. The measured aortic and myocardial pressures could be used as the model inputs. The flows and pressures determined by the model could be compared to the measured flows and pressures.

The technique of expanding the model to include the effects of a number of coronary vessels is a straightforward extension of the techniques developed herein. The level of sophistication would

be limited only by the amount of computer time and space available. A more sophisticated model could easily include the variations of myocardial pressure with depth. It would be a simple matter to take into account the varying lengths, diameters, and orientations of the coronary arteries. Effects of such diseases as atherosclerosis on coronary blood flow could be examined by simulating the effect of these diseases. In the case of atherosclerosis the arteries would be narrowed and the Young's modulus of the arteries increased. The utility of a representational model of the coronary circulation is evident and worthy of further research.

REFERENCES

- (1) A. C. Burton, Physiology and Biophysics of the Circulation. 2 ed. Chicago: Year Book Medical, 1972.
- (2) J. Grayson, J. W. Davidson, A. Fitzgerald-Finch, and C. Scott, "The functional morphology of the coronary microcirculation in the dog." Microvascular Research, vol. 8, pp. 20-43, 1974.
- (3) C. G. Caro, T. J. Pedley, R. C. Schroter, and W. A. Seed, The Mechanics of the Circulation. New York: Oxford University Press, 1978.
- (4) V. L. Streeter, "Stress distribution in the canine left ventricle during diastole and systole." Biophysical Journal, vol. 10, p. 357, 1970.
- (5) E. W. Merrill, "Rheology of blood." Physiological Reviews, vol. 49, no. 4, pp. 863-888, 1969.
- (6) M. R. Roach, "Biophysical analyses of blood vessel walls and blood flow." Annual Review of Physiology, vol. 39, pp. 51-71.
- (7) A. I. Katz, Y. Chen, and A. H. Moreno, "Flow through a collapsible tube: experimental analysis and mathematical models." Biophysical Journal, vol. 9, pp. 1261-1279, 1969.
- (8) J. Jelinek, "Hemodynamics of counterpulsation: the study of a lumped-parameter computer model." Journal of Biomechanics, vol. 5, pp. 511-519, 1972.
- (9) M. F. Snyder, V. C. Rideout, and R. J. Hillestad, "Computer modeling of the human systemic arterial tree." Journal of Biomechanics, vol. 1, pp. 341-353, 1968.

- (10) W. S. Kuklinski, "Closed loop control of intra-aortic balloon pumping: studies using a computer simulation and animal experiments," Ph. D. dissertation, Dep. Elec. Eng., University of Rhode Island, 1979.
- (11) E. O. Attinger and F. M. Attinger, "Frequency dynamics of peripheral vascular blood flow." Annual Review of Biophysics and Bioengineering, vol. 2, pp. 7-36, 1973.
- (12) V. C. Rideout and D. E. Dick, "Difference-differential equations for fluid flow in distensible tubes." IEEE Transactions on Biomedical Engineering, vol. 14, no. 3, pp. 171-177, July 1967.
- (13) W. Flugge, Stresses in Shells. Germany: Springer-Verlag OHG, 1960.
- (14) J. E. Gibson, Linear Elastic Theory of Thin Shells. New York: Pergamon Press, 1965.
- (15) F. M. White, Viscous Fluid Flow. New York: McGraw-Hill, 1974.
- (16) D. E. Gregg, E. M. Khouri, and C. R. Rayford, "Systemic and coronary energetics in the resting unanesthetized dog." Circulation Research, vol. 16, Feb. 1965.
- (17) B. Carnahan, H. A. Luther, and J. O. Wilkes, Applied Numerical Methods. New York: John Wiley & Sons, 1969.
- (18) H. J. Bartsch, Handbook of Mathematical Formulas. New York: Academic Press.

APPENDIX

Development of Subroutines

The elliptical capacitance (equation (32)) requires the evaluation of the integral

$$\int_0^{2\pi} r^3 d\phi$$

where r = radius of curvature of an ellipse

ϕ = angle with the x axis

This integral was evaluated using the repeated interval halving technique (17). If T_N is the computed estimate of the integral

$$\int_a^b f(x) dx$$

and T_N is based upon the composite trapezoidal rule, then the general recursion relation for T_N in terms of T_{N-1} is

$$T_N = \frac{1}{2} \left\{ T_{N-1} + \frac{b-a}{2^{N-1}} \sum_{\substack{i=1 \\ \Delta i=2}}^{2^N-1} f\left(a + \frac{(b-a)}{2^N} i\right) \right\} \quad (47)$$

$$\text{where } T_0 = \frac{b-a}{1} \left\{ \frac{1}{2} (f(a) + f(b)) \right\}$$

and N is the number of times the initial integration interval (a,b) has been halved to produce subintervals of length $L = (b-a)/2^N$.

The recursion relation of equation (47) can be used to compute the sequence $T_1, T_2, T_3, \dots, T_N$ once T_0 has been calculated. The function $f(x)$ need be evaluated just $2^N + 1$ times to compute the entire sequence.

The error term is

$$-\frac{(b-a)^3}{12(2)^{2N}} f''(\xi) \quad (48)$$

ξ in (a,b)

If $f(x)$ has a continuous and bounded second derivative on the interval (a,b) , equation (48) assures that the sequence $T_0, T_1, T_2, \dots, T_N$ converges to the true integral, assuming that no round off errors enter into the calculation.

The cube of the radius of curvature for an ellipse is evaluated by the function F. The integral is computed by the subroutine RIHINT.

When the section is in elliptical cross section the cross sectional area and circumference are known. It is imperative that the length of the major and minor axis be known to facilitate the calculation of the resistance, inertance, and capacitance. The expression for the circumference of an ellipse is (18)

$$C = 2\pi a \left\{ 1 - \left(\frac{1}{2}\right)^2 \left(\frac{a^2-b^2}{a^2}\right) - \left(\frac{1 \cdot 3}{2 \cdot 4}\right)^2 \left(\frac{a^2-b^2}{a^2}\right)^2 \left(\frac{1}{3}\right) - \left(\frac{1 \cdot 3 \cdot 5}{2 \cdot 4 \cdot 6}\right)^2 \left(\frac{a^2-b^2}{a^2}\right)^3 \left(\frac{1}{5}\right) - \dots \right\} \quad (49)$$

where C = circumference

a = length of the major axis

b = length of the minor axis

The expression for the area (A) of an ellipse is

$$A = \pi ab$$

Equation (49) may be written in terms of the cross sectional area and the major or minor axis. In this form the circumference is given by

$$C = \frac{2A}{b} \left\{ 1 - \left(\frac{1}{2}\right)^2 \left(\frac{A^2 - \pi^2 b^4}{A^2}\right) - \left(\frac{1 \cdot 3}{2 \cdot 4}\right)^2 \left(\frac{A^2 - \pi^2 b^4}{A^2}\right)^2 - \left(\frac{1}{3}\right) - \left(\frac{1 \cdot 3 \cdot 5}{2 \cdot 4 \cdot 6}\right)^2 \left(\frac{A^2 - \pi^2 b^4}{A^2}\right)^3 \right. \\ \left. \left(\frac{1}{5}\right) - \dots \right\} \quad (50)$$

Equation (50) will be abbreviated as

$$C = F(b) \quad (51)$$

Equation (51) may be written as

$$0 = F(b) - C \quad (52)$$

It then becomes necessary to find b such that equation (52) is satisfied. This is equivalent to finding the real root of equation (52). Knowing b allows a to be calculated by

$$a = \frac{A}{\pi b}$$

The technique for finding this real root employed in this program is the half-interval method (17). This method was applied for two reasons:

1. Equation (50) is not easily reduced to polynomial form thus making other root search techniques difficult to implement.
2. The half interval method provides a technique for assuring that the root is accurate within a specified range of uncertainty.

This technique is easily understood with a simple graphical illustration (Fig. 30). If values x_{L1} and x_{R1} are known, it gives a root such that $f(x_{L1})$ and $f(x_{R1})$ are opposite in sign. For a continuous function, the number $f\{(x_{L1} + x_{R1})/2\}$, which is the value of the function at the halfway point, will be either zero or have the sign of $f(x_{L1})$ or the sign of $f(x_{R1})$. If the value is not

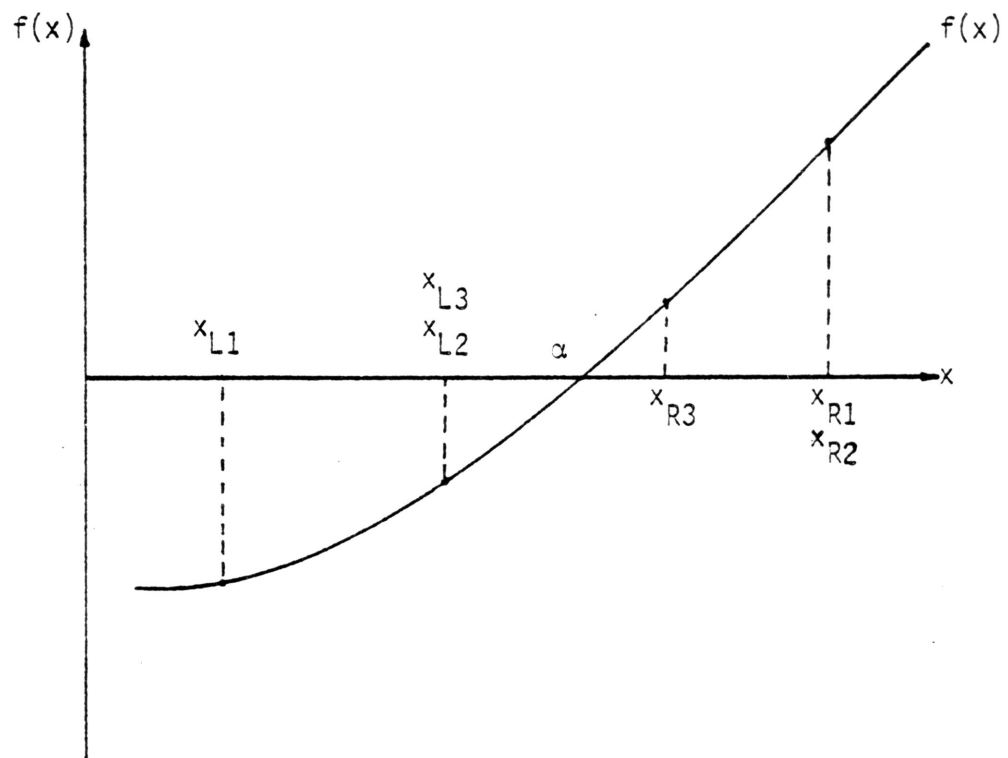


Fig. 30. Half-interval method.

zero, a second pair x_{L2} and x_{R2} can be chosen from the three numbers x_{L1} , x_{R1} , and $(x_{L1} + x_{R1})/2$ so that $f(x_{L2})$ and $f(x_{R2})$ are opposite in sign, while

$$|x_{L2} - x_{R2}| = \frac{1}{2}|x_{L1} - x_{R1}|$$

Continuing in this manner there is always a point α in the interval (x_{Lk}, x_{Rk}) for which $f(\alpha) = 0$.

If Δ_1 is the length of the starting interval, then the number n of interval-halving operations required to reduce the interval of uncertainty Δ_n is given by

$$n = \frac{\ln(\Delta_1/\Delta_n)}{\ln 2}$$

The calculation of

F(b)-C

is accomplished by the function ZCIRM. The major and minor axes are found using the half-interval root search technique in the subroutine AXES.

Program Listing

```

C
C      THIS PROGRAM MODELS THE EFFECT OF VENTRICULAR CONTRACTION ON
C      CORONARY BLOOD FLOW. A FLUID/ELECTRICAL ANALOG IS USED. A
C      CORONARY ARTERY IS DIVIDED INTO THREE SECTIONS. CHANGES IN
C      CROSS SECTIONAL AREA ARE DETERMINED BY COMPARING FLOW IN AND
C      OUT OF A SECTION. THE RATIO OF PRESENT CROSS SECTIONAL AREA
C      TO ORIGINAL CROSS SECTIONAL AREA DEFINES THE CROSS SECTIONAL
C      CONFIGURATION. THREE CONFIGURATIONS ARE POSSIBLE: CIRCULAR,
C      ELLIPTICAL AND DUMBELL. THE CONFIGURATION DETERMINATION
C      ALLOWS FOR THE CALCULATION OF THE FLUID RESISTANCE (R),
C      INDUCTANCE (L), AND CAPACITANCE (C) FOR THAT CROSS SECTIONAL
C      CONFIGURATION. THE ASSUMED HEART RATE IS 1 BEAT/SECOND. J
C      IS THE NUMBER OF ITERATIONS PER SECOND. ILM IS THE NUMBER
C      OF HEART BEATS TO BE RUN. RAD IS THE RADIUS OF THE CORONARY
C      ARTERY. DELZ IS THE LENGTH OF ONE OF THE THREE SECTIONS.
C      MU IS THE FLUID VISCOSITY. RHO IS THE FLUID DENSITY. NU IS
C      POISSON'S RATIO FOR THE ARTERY. E IS THE YOUNG'S MODULUS
C      FOR THE ARTERY. H IS THE THICKNESS OF THE VESSEL WALL.
C      RTERM IS THE RESISTANCE OF THE FOURTH TERMINATING SECTION.
C      DELUN IS THE INTERVAL OF UNCERTAINTY FOR THE ROOT SEARCH
C      TECHNIQUE. NMAX DETERMINES THE NUMBER OF INTERVAL HALVINGS
C      FOR THE INTEGRATION TECHNIQUE.
C
C      DIMENSION AF(3,100),PFA(4,100),QFA(4,100)
C      DOUBLE PRECISION P(4,2),Q(4,2),DA,DELZ,RTERM,AO,PI,RAD,MU,NU,
C      *E,H,RHO,T,AN(3),DELT,PE(3,2),PCAL(4),CIRCMO
C      COMMON AN,Q,P,DELT,PE,MU,DELZ,PI,RHO,NU,E,H,N
C
C      ..... PARAMETERS ARE SUPPLIED .....
C
C      DATA J/1000/
C      DATA ILM/30/
C      DATA RTERM/5.76D4/
C      DATA RAD/0.048D0/
C      DATA PI/3.1415D0/
C      DATA DELUN/0.00005/
C      DATA NMAX/10/
C      DATA DELZ/4.D0/
C      DATA MU/0.03D0/
C      DATA RHO/1.05D0/
C      DATA NU/0.5D0/
C      DATA E/5.D6/
C      DATA H/9.6D-3/
C      M=0
C
C      ..... INITIAL CONDITIONS ARE ESTABLISHED .....
C
C      DO 95 JJ=1,4
C      P(JJ,1)=10.D4
C      Q(JJ,1)=0.D4
C 95  CONTINUE
C      DO 69 KK=1,3
C 69  PE(KK,1)=0.
C
C      ..... ORIGINAL AREA IS CALCULATED .....
C
C      AO=PI*RAD**2
C      AN(1)=AO
C      AN(2)=AO
C      AN(3)=AO
C
C      ..... ORIGINAL CIRCUMFERENCE IS CALCULATED .....
C
C      CIRCMO=2.D0*DSQRT(AO*PI)
C
C      ..... LENGTH OF TIME INCREMENT IS DETERMINED .....
C
C      DELT=1.00/J

```

```

C
C      ..... UNITS ARE PRINTED .....
C      WRITE(6,15)
15  FORMAT(' ', '(P)=GM*CM/SEC**4',5X, '(Q)=CM**3/SEC',5X, '(A)=CM**2')
C
C      ..... NUMBER OF ITERATIONS PER SECOND IS PRINTED .....
C      WRITE(6,20) J
20  FORMAT(' ', 'THE NUMBER OF ITERATIONS PER SECOND IS ',I3,'.')
C
C      ..... LOOP DETERMINING NUMBER OF HEART BEATS .....
C      DO 12 IFOR=1,ILIM
C
C      ..... LOOP DETERMINING NUMBER OF INTERVALS .....
C      DO 11 INTER=1,J
C
C      ..... TOTAL ELAPSED TIME IS DETERMINED .....
C      T=(INTER-1.D0)*DELT
C
C      ..... SUBROUTINE PRESS CALLED TO DETERMINE
C      AORTIC AND VENTRICULAR PRESSURES .....
C      CALL PRESS(T,PCAL)
C
C      ..... PRESSURES ARE CONVERTED FROM
C      MM OF HG TO DYNE/CM**2 .....
C      PE(1,2)=PCAL(1)*1.333D3
C      PE(2,2)=PCAL(2)*1.333D3
C      PE(3,2)=PCAL(3)*1.333D3
C      P(1,2)=PCAL(4)*1.333D3
C
C      ..... PRESSURE AND FLOW IN EACH SECTION
C      IS DETERMINED .....
C      DO 10 N=1,4
C      IF(N.EQ.4) GOTO 5
C
C      ..... CROSS SECTIONAL CONFIGURATION
C      IS DETERMINED .....
C      IF(AN(N)/AO.GE.0.9D0)CALL CIRCLE
C      IF(AN(N)/AO.GT.0.3D0.AND.AN(N)/AO.LT.0.9D0)CALL ELLIPS(CIRCMD,
C      *DELUN,NMAX)
C      IF(AN(N)/AO.LE.0.3D0) CALL DUMBEL
C      GOTO 10
C
C      ..... CALCULATION OF FLOW IN TERMINAL SECTION .....
C      5 Q(4,2)=P(4,2)/RTERM
C      10 CONTINUE
C
C      ..... FINAL ARRAYS FOR PLOTTING (PFA,QFA,AF) ARE
C      ESTABLISHED. PLOTLP IS A LIBRARY LINE
C      PRINTER PLOTTING SUBROUTINE .....
C      IF(IFOR.NE.ILIM)GOTO 6
C      IF((INTER/10)*10.NE.INTER) GOTO 6
C      M=M+1
C      DO 13 I=1,4
C      PFA(I,M)=P(I,1)
C      QFA(I,M)=Q(I,1)
13  CONTINUE
C      DO 22 I=1,3
C      AF(I,M)=AN(I)
22  CONTINUE
C      6 CONTINUE
C      DO 9 K=1,3
C
C      ..... CHANGE IN CROSS SECTIONAL AREA (DA)
C      IS DETERMINED .....
C      DA=(Q(K,2)-Q(K+1,2))*DELT/DELZ
C
C      ..... NEW CROSS SECTIONAL AREA DETERMINED .....
C      AN(K)=AN(K)+DA
C

```

```

C
C      .... LOWER AREA LIMIT SET ....
C      IF(AN(K).LT.0.158D-2)AN(K)=0.158D-2
3  CONTINUE
C
C      .... PRESENT VALUES LOADED INTO
C      PAST VALUES ....
      DO 23 K=1,4
      P(K,1)=P(K,2)
23  Q(K,1)=Q(K,2)
      DO 1  LL=1,3
1   PE(LL,1)=PE(LL,2)
18  CONTINUE
11  CONTINUE
12  CONTINUE
50  CONTINUE
C
C      .... PARAMETERS FOR PLOTLP ESTABLISHED
C      AND PLOTLP CALLED ....
      XSTART=0.0
      XINC=0.01
      NPLOTS=4
      NPTS=100
      ND=4
      WRITE (6,30)
      CALL PLOTLP(XSTART,XINC,PPA,NPLOTS,NPTS,ND)
      WRITE (6,30)
      CALL PLOTLP(XSTART,XINC,QFA,NPLOTS,NPTS,ND)
      WRITE (6,30)
      NPLOTS=3
      ND=3
      CALL PLOTLP(XSTART,XINC,AF,NPLOTS,NPTS,ND)
30  FORMAT(1H1)
      STOP
      END
C
C      SUBROUTINE PRESS DETERMINES AORTIC PRESSURE P(4) AND THE
C      SECTIONAL VENTRICULAR PRESSURES P(1), P(2), P(3). T IS
C      THE TIME.
C
      SUBROUTINE PRESS(T,P)
      DOUBLE PRECISION T,P(4)
      IF(T.GE.0..AND.T.LT.0.25)P(1)=20.8*T
      IF(T.GE.0.25.AND.T.LT.0.3)P(1)=194.*T-43.3
      IF(T.GE.0.3.AND.T.LT.0.37)P(1)=1215.7*T-349.81
      IF(T.GE.0.37.AND.T.LT.0.5)P(1)=20.*DSIN(3.1415*(T-0.37)/0.26)+
*100.
      IF(T.GE.0..AND.T.LT.0.2)P(2)=20.8*T+1.04
      IF(T.GE.0.2.AND.T.LT.0.25)P(2)=194.*T-33.6
      IF(T.GE.0.25.AND.T.LT.0.32)P(2)=1215.7*T-289.025
      IF(T.GE.0.32.AND.T.LT.0.45)P(2)=20.*DSIN(3.1415*(T-0.32)/0.26)+
*100.
      IF(T.GE.0.45.AND.T.LT.0.5)P(2)=120.
      IF(T.GE.0..AND.T.LT.0.15)P(3)=20.8*T+2.08
      IF(T.GE.0.15.AND.T.LT.0.20)P(3)=194.*T-23.9
      IF(T.GE.0.20.AND.T.LT.0.27)P(3)=1215.7*T-228.24
      IF(T.GE.0.27.AND.T.LT.0.40)P(3)=20.*DSIN(3.1415*(T-0.27)/0.26)+
*100.
      IF(T.GE.0.4.AND.T.LT.0.5)P(3)=120.
      IF(T.GE.0.5.AND.T.LT.0.63)P(1)=P(2)=P(3)=20.*DSIN(3.1415*(T-0.37)/
*0.26)+100.
      IF(T.GE.0.63.AND.T.LT.0.7)P(1)=P(2)=P(3)=-1290.*T+912.7
      IF(T.GE.0.7.AND.T.LT.0.77)P(1)=P(2)=P(3)=-138.6*T+106.72
      IF(T.GE.0.77)P(1)=P(2)=P(3)=0.
      IF(T.GE.0.95.AND.T.LT.1.0)P(2)=20.8*T-19.76
      IF(T.GE.0.9.AND.T.LT.1.0)P(3)=20.8*T-18.72

```

```

IF(T.GE.0.1.AND.T.LT.0.35)P(4)=-33.06*T+91.
IF(T.GE.0.35.AND.T.LT.0.69)P(4)=40.9*DSIN(3.1415*(T-0.35)/0.30)+
*79.1
IF(T.GE.0.69)P(4)=-30.*T+121.
RETURN
END

```

```

C
C      SUBROUTINE CIRCLE COMPUTES THE FLUID RESISTANCE (R),
C      INDUCTANCE (L), AND CAPACITANCE (C) FOR A CIRCULAR CROSS
C      SECTION. THE PRESENT VALUES OF PRESSURE (P) AND FLOW (Q)
C      ARE THEN DETERMINED. RADDCIR IS THE RADIUS OF THE CIRCULAR
C      CROSS SECTION.
C

```

```

SUBROUTINE CIRCLE
DOUBLE PRECISION R,L,C,AN(3),Q(4,2),P(4,2),DELT,PE(3,2)
*,MU,DELZ,PI,RHO,NU,RADDCIR,E,H
COMMON AN,Q,P,DELT,PE,MU,DELZ,PI,RHO,NU,E,H,N
RADDCIR=DSQRT(AN(N)/PI)
R=(8.D0*MU*DELZ)/(PI*RADDCIR**4)
L=(9.D0*RHO*DELZ)/(4.D0*PI*RADDCIR**2)
C=(DELZ*(1-NU**2)*2.D0*PI*RADDCIR**3)/(E*H)
P(N+1,2)=(Q(N,1)-Q(N+1,1))*(1.D0/C)*DELT+P(N+1,1)+PE(N,2)-PE(N,1)
Q(N,2)=(1.D0/L)*(P(N,1)-R*Q(N,1)-P(N+1,1))*DELT+Q(N,1)
RETURN
END

```

```

C
C      SUBROUTINE ELLIPS COMPUTES THE FLUID RESISTANCE (R),
C      INDUCTANCE (L), AND CAPACITANCE (C) FOR AN ELLIPTICAL CROSS
C      SECTION. THE PRESENT VALUES OF PRESSURE (P) AND FLOW (Q)
C      ARE THEN COMPUTED.
C

```

```

SUBROUTINE ELLIPS(CIRCMO,DELUN,NMAX)
DOUBLE PRECISION R,L,C,AN(3),Q(4,2),P(4,2),DELT,PE(3,2)
*,MU,DELZ,PI,RHO,NU,CIRCMO,A,B,R3INT,E,H
COMMON AN,Q,P,DELT,PE,MU,DELZ,PI,RHO,NU,E,H,N

```

```

C
C      ..... SUBROUTINE AXES DETERMINES THE
C      LENGTH OF THE MAJOR AND MINOR AXES (A,B) .....
CALL AXES(A,B,DELUN,CIRCMO,AN,N)

```

```

C
C      ..... SUBROUTINE RIHINT EVALUATES THE
C      INTEGRAL OF THE RADIUS OF CURVATURE
C      CUBED (R3INT) .....
CALL RIHINT(R3INT,A,B,NMAX,PI)
R=(4.D0*MU*DELZ*(A**2+B**2))/(PI*(A**3*B**3))
L=(9.D0*RHO*DELZ)/(4.D0*PI*A*B)
C=(DELZ*(1-NU**2)*R3INT)/(E*H)
P(N+1,2)=(Q(N,1)-Q(N+1,1))*(1.D0/C)*DELT+P(N+1,1)+PE(N,2)-PE(N,1)
Q(N,2)=(1.D0/L)*(P(N,1)-R*Q(N,1)-P(N+1,1))*DELT+Q(N,1)
RETURN
END

```

```

C
C      SUBROUTINE DUMBEL COMPUTES THE FLUID RESISTANCE (R),
C      INDUCTANCE (L), AND CAPACITANCE (C) FOR A DUMBELL CROSS
C      SECTION. THE PRESENT VALUES OF PRESSURE (P) AND FLOW (Q)
C      ARE DETERMINED. RADUM IS THE RADIUS OF A DUMBELL LOBE.
C

```

```

SUBROUTINE DUMBEL
DOUBLE PRECISION R,L,C,AN(3),Q(4,2),P(4,2),DELT,PE(3,2)
*,MU,DELZ,PI,RHO,NU,RADUM,E,H
COMMON AN,Q,P,DELT,PE,MU,DELZ,PI,RHO,NU,E,H,N
RADUM=DSQRT(AN(N)/2.D0/3.1415D0)
R=(8.D0*MU*DELZ)/(PI*RADUM**4)
L=(9.D0*RHO*DELZ)/(4.D0*PI*RADUM**2)
C=(DELZ*(1.D0-NU**2)*2.D0*PI*RADUM**3)/(E*H)
P(N+1,2)=(Q(N,1)-Q(N+1,1))*DELT*0.5D0*1.D0/C+P(N+1,1)+PE(N,2)-
*PE(N,1)
Q(N,2)=(P(N,1)-R/2.D0*Q(N,1)-P(N+1,1))*2.D0*DELT*(1.D0/L)+Q(N,1)
RETURN
END

```



```

C
C      SUBROUTINE RIHINT EVALUATES THE INTEGRAL OF THE RADIUS OF
C      CURVATURE CUBED OF AN ELLIPSE.  THE INTEGRAL EXTENDS
C      FROM 0. TO 2*PI.  SYMMETRY ALLOWS THE INTEGRAL
C      TO BE EVALUATED FROM 0. TO PI/2.  THIS INTEGRAL IS THEN
C      MULTIPLIED BY 4.  THE INTEGRAL FROM 0. TO PI/2.
C      IS T(NMAX+1).
C
C      SUBROUTINE RIHINT(R3INT,A,B,NMAX,PI)
C      DOUBLE PRECISION F,FR,R3INT,A,B,T(101),PI
C
C      ..... FIRST INTEGRAL APPROXIMATION .....
C      T(1)=(PI/2.00)*0.5D0*(F(A,B,0.00)+F(A,B,PI/2.00))
C
C      ..... INTERVAL HALVED REPEATEDLY .....
C      DO 2 L=1,NMAX
C      T(L+1)=0.000
C      FR=(PI/2.00)/2.00**L
C      IMAX=2**L-1
C      DO 1 I=1,IMAX,2
C      1 T(L+1)=T(L+1)+F(A,B,FLOAT(I)*FR)
C      2 T(L+1)=T(L)/2.00+(PI/2.00)*T(L+1)/2.00**L
C
C      ..... INTEGRAL (R3INT) COMPUTED .....
C      R3INT=4.00*T(NMAX+1)
C      RETURN
C      END
C
C      SUBROUTINE AXES DETERMINES THE LENGTH OF THE MAJOR AND MINOR
C      AXES (A,B) OF AN ELLIPSE GIVEN A CIRCUMFERENCE AND AREA.
C      THE HALF INTERVAL ROOT SEARCH METHOD IS USED.
C
C      SUBROUTINE AXES(A,B,DELUN,CIRCMO,AN,N)
C      DOUBLE PRECISION ZL,ZCIRCM,ZR,CIRCZL,ZHALF,CIRZHF,A,B,AN(3),
C      *CIRCMO
C
C      ..... NUMBER OF ITERATIONS DETERMINED .....
C      ITER=ALOG(0.05/DELUN)/ALOG(2.0)+1.0
C
C      ..... ESTABLISH INTERVAL WITHIN WHICH ROOT LIES .....
C      ZL=0.00500
C      1 IF(ZCIRCM(ZL,CIRCMO,AN,N)*ZCIRCM(ZL+0.05D0,CIRCMO,AN,N).LT.0.00)
C      *GOTO 3
C      ZL=ZL+0.05D0
C      GOTO 1
C      3 ZR=ZL+0.05D0
C      CIRCZL=ZCIRCM(ZL,CIRCMO,AN,N)
C
C      ..... BEGIN HALF INTERVAL ITERATION .....
C      DO 6 I=1,ITER
C      ZHALF=(ZL+ZR)/2.0
C      CIRZHF=ZCIRCM(ZHALF,CIRCMO,AN,N)
C
C      ..... CHOOSE SUBINTERVAL CONTAINING THE ROOTS .....
C      IF(CIRZHF*CIRCZL.LE.0.000) GOTO 5
C      ZL=ZHALF
C      CIRCZL=CIRZHF
C      GOTO 6
C      5 ZR=ZHALF
C      6 CONTINUE
C
C      ..... DETERMINE MAJOR AND MINOR AXES .....
C      7 B=(ZL+ZR)/2.000
C      A=AN(N)/(3.1415D0*B)
C      RETURN
C      END

```

```

C
C      FUNCTION ZCIRCM DETERMINES THE DIFFERENCE BETWEEN THE
C      CIRCUMFERENCE OF AN ELLIPSE AND THE ORIGINAL CIRCUMFERENCE
C      GIVEN AN AXIS LENGTH AND AREA. THE EXPRESSION RELATING AN
C      AXIS AND AREA TO CIRCUMFERENCE IS AN INFINITE SERIES. THIS
C      SERIES IS EVALUATED TO TEN TERMS.
C

```

```

      FUNCTION ZCIRCM(Z,CIRCMO,AN,N)
      DOUBLE PRECISION S,P1,D,A,B,P2,ZCIRCM,Z,CIRCMO,AN(3)
      S=1.D0
      P1=1.D0
      D=(AN(N)**2-3.1415D0**2*Z**4)/AN(N)**2
      DO 15 I=1,10
      P1=P1*((2*I-1)/(2*I))**2
      P2=P1*D**I*(1/(2*I-1))
15  S=S-P2
      ZCIRCM=2.D0*AN(N)/Z*S-CIRCMO
      RETURN
      END

```

```

C
C      FUNCTION F EVALUATES THE EXPRESSION FOR THE RADIUS OF
C      CURVATURE CUBED OF AN ELLIPSE. A AND B ARE THE MAJOR AND
C      MINOR AXES. PHI IS THE ANGLE WITH THE X AXIS.
C

```

```

      FUNCTION F(A,B,PHI)
      DOUBLE PRECISION A,B,PHI,F
      F=(A**6*B**6)/((A**2*DSIN(PHI)**2+B**2*DCOS(PHI)**2)**4.5)
      RETURN
      END

```